

# Hadronic vacuum polarization to three loops in chiral perturbation theory

---

**Laurent Lellouch,<sup>a</sup> Alessandro Lupo,<sup>a</sup> Mattias Sjö,<sup>a</sup> Kálmán Szabo,<sup>b,c</sup> and Pierre Vanhove<sup>d</sup>**

<sup>a</sup>*Aix Marseille Univ, Université de Toulon, CNRS, CPT, Marseille, France*

<sup>b</sup>*Department of Physics, University of Wuppertal, D-42119 Wuppertal, Germany*

<sup>c</sup>*Jülich Supercomputing Centre, Forschungszentrum Jülich, D-52428 Jülich, Germany*

<sup>d</sup>*Institut de Physique Théorique, Université Paris-Saclay, CEA, CNRS,  
F-91191 Gif-sur-Yvette Cedex, France*

**ABSTRACT:** Hadronic vacuum polarization at low virtualities limits the precision of experimental tests of the standard model via important physical observables. Here we compute that effect in two-flavor chiral perturbation theory to three loops. Among the master integrals that describe the amplitude, six are elliptic functions of the momentum. Of these five are new to this work, although all can be related to the three-loop sunset integral. The renormalizability of the amplitude hinges on relations between the master integrals that were not previously known and that are not consequences of the integration-by-parts reduction. Our result is intended to serve as a starting point for phenomenological calculations, as well as the computation of finite-volume corrections in lattice QCD.

---

## Contents

<b>1</b>	<b>Introduction</b>	<b>1</b>
<b>2</b>	<b>Theoretical background</b>	<b>4</b>
2.1	The ChPT Lagrangian	5
2.2	Renormalization	6
2.3	Diagrams	6
2.4	Mass and decay constant	7
<b>3</b>	<b>The loop integrals</b>	<b>9</b>
3.1	Loop integral manipulations	9
3.2	Master integrals of $\Pi^{\mu\nu}(q^2)$ at three-loop order	10
<b>4</b>	<b>Results</b>	<b>12</b>
4.1	Expressions for the HVP	13
4.2	$N^3LO$ renormalization	15
4.3	Dependence on the LECs	15
<b>5</b>	<b>Conclusions and outlook</b>	<b>16</b>
<b>A</b>	<b>More on loop integral manipulations</b>	<b>17</b>
A.1	Differential equations	17
A.2	Tarasov's dimensional shift	18
A.3	Schouten relations	20
<b>B</b>	<b>Differential equations for the master integrals</b>	<b>23</b>
B.1	Differential equations for tadpoles and bubbles	23
B.2	Differential equations for $E_1, E_2$ and $E_3$	23
B.3	Differential equation for $E_4$	24
B.4	Differential equations for $E_5$ and $E_6$	24
B.5	Initial conditions	25
<b>C</b>	<b>Dimension-shifting relations</b>	<b>26</b>
C.1	Dimension shifting for the master $E_0$	26
C.2	Dimension shifting for the masters $E_1, E_2$ and $E_3$	27
C.3	Dimension shifting for the master $E_4$	28
C.4	Dimension shifting for the masters $E_5$ and $E_6$	28
<b>D</b>	<b>Expressions for the master integrals in <math>d = 4 - 2\epsilon</math> dimensions</b>	<b>31</b>
D.1	The one-loop bubble in $d = 4 - 2\epsilon$	31
D.2	The tadpole-bubble products in $d = 4 - 2\epsilon$ dimensions	32
D.3	The master integral $E_0$ in $d = 4 - 2\epsilon$	33

D.4	The master integrals $E_1$ , $E_2$ and $E_3$ in $d = 4 - 2\epsilon$	33
D.5	The master integral $E_4$ in $d = 4 - 2\epsilon$	34
D.6	The master integral $E_5$ in $d = 4 - 2\epsilon$	34
D.7	The master integral $E_6$ at $d = 4 - 2\epsilon$	36
<b>E</b>	<b>Expressions for the master integrals in two dimensions</b>	<b>37</b>
<b>F</b>	<b>Unsubtracted expressions for the HVP</b>	<b>38</b>
<b>G</b>	<b>Implementation details</b>	<b>39</b>
	<b>References</b>	<b>40</b>

---

## 1 Introduction

The propagation of photons in the vacuum is modified by quantum fluctuations of the quark and gluon fields. This phenomenon is known as hadronic vacuum polarization (HVP). At low virtualities, our current knowledge of HVP limits the precision of experimental tests of the standard model via important observables such as the muon anomalous magnetic moment [1] or the value of the electromagnetic coupling at the electroweak scale [2]. To align the standard-model prediction for the muon  $g - 2$  with the current experimental uncertainty [1], the precision of the HVP contribution must improve by a factor of 4 relative to the world average of [3] or by a factor of 2 compared to the result in ref. [4]. Furthermore, stringent tests of the standard model via precision electroweak observables at future facilities such as CERN’s FCC-ee require reducing uncertainties by a factor of 3 on the running of  $\alpha$  at low virtualities [2]. To various degrees, HVP also enters the computation of quantities such as the anomalous magnetic moments of the electron and the  $\tau$ , as well as the ground-state hyperfine splitting of muonium and muonic helium (see e.g. ref. [5]).

At low energies, the challenge of computing HVP stems from the fact that quark and gluon interactions are highly non-linear and not amenable to the usual perturbative methods of quantum field theory (QFT): the strong interaction, described by quantum chromodynamics (QCD), is nonperturbative in that regime. There are two main approaches to addressing this challenge: massively parallel numerical simulations in a discretized version of QCD known as lattice QCD, and a data-driven approach. The latter combines the measurement of the  $e^+e^- \rightarrow \text{hadrons}$  cross section as a function of center-of-mass energy with fundamental features of relativistic QFT, such as unitarity and analyticity properties of two-point Green’s functions (see e.g. ref. [3] for a review).

A third approach is Chiral Perturbation Theory (ChPT) [6, 7]. ChPT is the low-energy effective field theory of QCD and, as such, is a key tool for studying hadronic interactions at low energies. While the predictive power of this approach is limited by the appearance of an increasing number of *a priori* unknown couplings at each new loop order

(low-energy constants, LECs), it does constrain the functional form of strong-interaction observables at low energies. In particular, it provides important information about the very low-energy QCD contributions to HVP that are dominated by two-pion contributions. This information can then be combined with the predictions of the main approaches to improve their accuracy. Here we present a calculation of those contributions to three loops in SU(2) ChPT [6].

One motivation for this calculation is to have a precise, model-independent determination of the finite-volume corrections that have to be applied to lattice results for quantities sensitive to long-distance HVP effects, such as the HVP contribution to the muon anomalous magnetic moment. Other model-independent approaches have also been proposed.<sup>1</sup> It is understood that finite-volume effects arise from long-distance, low-energy hadronic fluctuations, making SU(2) ChPT the natural framework to describe them [13]. Intuitively, the lightest propagating states will be the most sensitive to the finite spacetime boundaries, since they have the slowest rate of exponential decay with the spatial size  $L$  of the lattice. In the case of the isospin-1 channel, which is the largest part of the HVP contribution to the muon  $g - 2$ , these are states of two pions.

Finite-volume effects on the HVP contribution to the muon  $g - 2$  have been computed to one [14] and two [15, 16] loops. Assuming a geometric progression of these effects, the three-loop contribution and its uncertainty can be estimated, with the latter taken to be the sum of the remainder of the series. Using the results in ref. [16], one obtains  $(17.9 \pm 1.0) \times 10^{-10}$  for lattices of spatial (and temporal) extent  $L = 6.3$  fm ( $T = 2L/3$ ) that are typical of those used in state-of-the-art computations. This result is fully compatible with the direct lattice determination of that correction [16], but with an uncertainty that is 2.5 times smaller. Moreover, three loops is the first order in ChPT at which this uncertainty is smaller—by a factor of 1.5—than the one on the current world average of measurements of the muon  $g - 2$  [1], guaranteeing that this uncertainty is not a limiting factor in testing the Standard Model via this muon property. Of course, such a determination will require knowledge of a number of LECs. However, as discussed later, at three loops only six combinations of LECs contribute (three each from the NLO [6] and NNLO [17] Lagrangians), all of which can be determined from quantities such as the pion vector form factor at two loops.<sup>2</sup>

In the meantime, a precise lattice-plus-data-driven determination of the HVP contribution to  $a_\mu$  was obtained in [4]. In that approach, FVEs were reduced by a factor of roughly 2 and their uncertainty by approximately 3. This means that two-loop ChPT should be sufficient to reach the precision required by experiment. Nevertheless, a three-loop determination would provide an important cross-check of the corresponding uncertainty estimate. Moreover, a number of lattice collaborations are currently calculating the HVP contribution to  $a_\mu$  fully on the lattice [18–20] and for those the improvement brought by a three-loop calculation is relevant. In addition, such a calculation will reduce the uncertainty on lattice calculations of the low-energy running of  $\alpha$ .

---

<sup>1</sup>These are the Hansen-Patella method [8, 9] and the Meyer-Lellouch-Lüscher approach [10–12].

<sup>2</sup>In ref. [13] it is shown that a new counterterm involving muon fields is needed in the three-loop ChPT computation of  $a_\mu$ . However, because it is a contact term, it will only contribute to the FVEs on  $a_\mu$  to four loops. Moreover, no such counterterm is needed in the computation of the HVP function itself.

As a first step in computing those FVEs, we calculate here HVP in infinite volume to three loops in ChPT. Beyond the determination of FVEs, the results of this calculation are interesting in and of themselves. They not only allow the study of the slope, but also of the curvature and turnaround of the HVP function for spacelike momenta. In the timelike region, its imaginary part not only describes the interference between the one- [6] and two-loop [21] pion form-factor contributions to the  $e^+e^- \rightarrow \pi^+\pi^-$  cross section, but also the four-pion contribution, which is absent at lower orders. Moreover, it is only the second three-loop ChPT calculation performed and therefore pushes the envelope of such computations.<sup>3</sup>

The evaluation of the three-loop amplitude presented in this work requires state-of-the-art integration techniques of Feynman integrals and the use of new identities between master integrals, which are not derivable from the commonly used integration-by-part algorithms, and which were previously unknown. The one- and two-loop contributions to HVP only involve logarithms and polylogarithms, while the three-loop amplitude leads to elliptic integrals.

The elliptic master integrals needed in this work correspond to two-point functions with a single mass and no massless internal propagators. Using Tarasov dimension shifting relations [23], the elliptic master integrals are reduced to integrals in two dimensions that are both ultraviolet and infrared finite. Compared to previous three-loop computations in other theories, the fact that all internal lines are massive here leads to new elliptic master integrals that were unknown in the literature. All the needed elliptic master integrals can be obtained by differentiation or integration of the three-loop sunset integral in two dimensions. This integral arises in several precision calculations of the standard model [24, 25], quark and gluon self-energies [26], QED calculations [27–29] and in Higgs boson decay amplitudes [30]. It has been the subject of many studies, including refs. [31–35].

Using the algorithms developed in ref. [36, 37], we give the differential equations satisfied by the new elliptic master integrals. The resolution of these differential equations provides fast and high precision evaluations of the master integral in the complex energy plane, and a complete control of the theoretical uncertainties at this order in ChPT. The renormalization of the ultraviolet divergences of the three-loop amplitude is obtained thanks to the derivation of new relations between the elliptic master integrals evaluated in two dimensions. These relations are not a consequence of integration-by-part identities as they arise in fixed spacetime dimension. We provide two ways of deriving them, one based on the familiar Schouten identities [38] and another using the differential equations satisfied by the master integrals.

While we give an analytic derivation of these elliptic master integrals here, we defer details concerning their numerical implementation to forthcoming work [39]. Likewise, due to the complexity of the present calculation, we focus here on the computation of the three-loop HVP amplitude itself, postponing phenomenological applications and the

---

<sup>3</sup>The only other one that we know of is the three-loop computation of the pion mass and decay constant by Bijnens & Hermansson-Truedsson [22].

computation of finite-volume effects to later work.

We conclude this introduction with a summary of earlier ChPT HVP calculations. It was calculated at one-loop order in Gasser & Leutwyler's original ChPT papers [6, 7]. The two-loop calculation was performed by Golowich & Kambor [40] and then at greater generality by Bijnens et al. [41, 42]. Few calculations have been carried out to three-loop order in ChPT. As mentioned above, to the best of our knowledge, there is only this work and the pion mass and decay constant calculated by Bijnens & Hermansson-Truedsson [22]. Reproduction of the results of refs. [22, 42], whose FORM [43, 44] implementations have been made available to us, served as helpful verification throughout the present calculation.

The remainder of this paper is structured as follows. Sec. 2 describes the relevant theoretical background and lists the Feynman diagrams. Sec. 3 is devoted to the treatment of the loop integrals, with lengthy expressions and further mathematical details in secs. A to E. We present the results in sec. 4, with further results in sec. F. A description of how the calculations were implemented can be found in sec. G, along with links to our codes.

## 2 Theoretical background

The basic quantity of interest is the vacuum polarization

$$\Pi^{\mu\nu}(q) := \int d^4x e^{iqx} \langle 0 | T\{j^\mu(x)j^\nu(0)\} | 0 \rangle, \quad (2.1)$$

where  $j_\mu(x)$  is the electromagnetic current. HVP consists of the hadronic contributions to  $\Pi^{\mu\nu}(q)$ , i.e., those where the right-hand side is computed from some model of hadrons, for which we use two-flavor ChPT as described in detail below. From now on, we will assume that  $\Pi^{\mu\nu}(q)$  contains only this hadronic part.

As a rank-2 tensor depending on a single four-vector  $q^\mu$ , Lorentz invariance dictates that  $\Pi^{\mu\nu}(q)$  can be projected onto just two orthogonal structures,

$$\Pi^{\mu\nu}(q) = (q^\mu q^\nu - q^2 \eta^{\mu\nu}) \Pi_T(q^2) + q^\mu q^\nu \Pi_L(q^2), \quad (2.2)$$

where (in  $d$  dimensions with  $\eta^{\mu\nu} \eta_{\mu\nu} = d$ )

$$\Pi_L(q^2) := \frac{1}{(q^2)^2} q_\mu q_\nu \Pi^{\mu\nu}(q), \quad \Pi_T(q^2) := \frac{1}{1-d} \left[ \frac{1}{q^2} \eta_{\mu\nu} \Pi^{\mu\nu}(q) - \Pi_L(q^2) \right] \quad (2.3)$$

are its longitudinal and transverse components, respectively. By the Ward–Takahashi identity,  $\Pi_L(q^2) = 0$ .<sup>4</sup>

---

<sup>4</sup>Most individual Feynman diagrams contributing to  $\Pi^{\mu\nu}(q)$  possess a longitudinal component, and the vanishing of  $\Pi_L(q^2)$  only becomes manifest after summing all diagrams and performing the master integral reduction (see sec. 3). Therefore, the Ward–Takahashi identity is a powerful sanity check on our calculations, ruling out most possible errors such as missing diagrams, erroneous symmetry factors, malformed Feynman rules, or misconfigured master integral reduction.

## 2.1 The ChPT Lagrangian

We use two-flavor ChPT in the isospin limit, describing the low-energy dynamics of a  $SU(2)$  triplet of pion fields of mass  $M_\pi$  coupled to an external, non-dynamical photon field  $A_\mu$ . We need the Lagrangian to the first four orders in the chiral power counting,

$$\mathcal{L}_{\text{ChPT}} = \mathcal{L}_{\text{LO}} + \mathcal{L}_{\text{NLO}} + \mathcal{L}_{\text{NNLO}} + \mathcal{L}_{\text{N}^3\text{LO}} + \dots \quad (2.4)$$

The pions are contained in a matrix field  $U$  which we parametrize as

$$U = \frac{i\Phi}{F_0\sqrt{2}} + \sqrt{1 - \frac{\langle\Phi^2\rangle}{4F_0^2}}, \quad (2.5)$$

where  $F_0$  is the bare pion decay constant and  $\Phi = \sum_i \phi^i \sigma^i$  is the matrix of pion fields. We normalize our Lie algebra as  $\langle\sigma^i \sigma^j\rangle = \delta^{ij}$ , where  $\langle\cdot\cdot\cdot\rangle$  denotes an  $SU(2)$  trace. The same physical results are obtained from any parametrization that is equivalent to eq. (2.5) up to  $\mathcal{O}(\Phi^2)$ , such as  $U = \exp(i\Phi/F_0\sqrt{2})$ .

The leading Lagrangian is

$$\mathcal{L}_{\text{LO}} = \frac{F_0^2}{4} \langle D_\mu U (D^\mu U)^\dagger + \chi U^\dagger + U \chi^\dagger \rangle, \quad (2.6)$$

featuring the covariant derivative  $D_\mu U := \partial_\mu U - ir_\mu U + iU\ell_\mu$ . In this calculation, the chiral gauge fields are simply  $\ell_\mu = r_\mu = A_\mu Q$  where  $Q = \frac{e}{3} \text{diag}(+2, -1)$  is the quark charge matrix. Likewise,  $\chi$ , which contains the quark mass matrix, is simply the bare pion mass  $M_0$ . However, we retain  $\ell_\mu, r_\mu$  and  $\chi$  to preserve the manifestly chiral-invariant appearance of the Lagrangian. We also keep  $\ell_\mu$  and  $r_\mu$  because the axial current, proportional to  $r_\mu - \ell_\mu$ , determines the pion decay constant which appears in our calculation (see sec. 2.4).

The next-to-leading Lagrangian is (following ref. [6] but using somewhat modernized notation)<sup>5</sup>

$$\begin{aligned} \mathcal{L}_{\text{NLO}} = & \frac{l_1}{4} \langle D_\mu U (D^\mu U)^\dagger \rangle^2 + \frac{l_2}{4} \langle D_\mu U (D_\nu U)^\dagger \rangle \langle D^\mu U (D^\nu U)^\dagger \rangle + \frac{l_3}{16} \langle \chi U^\dagger + U \chi^\dagger \rangle^2 \\ & + \frac{l_4}{2} \langle D_\mu \chi^\dagger D^\mu U \rangle + l_5 \langle U^\dagger F_R^{\mu\nu} U F_{L\mu\nu} \rangle + i \frac{l_6}{2} [\langle F_R^{\mu\nu} U_\mu U_\nu^\dagger \rangle + \langle F_L^{\mu\nu} U_\mu^\dagger U_\nu \rangle] \\ & - 2h_2 \langle F_R^{\mu\nu} F_{R\mu\nu} F_L^{\mu\nu} F_{L\mu\nu} \rangle + \dots, \end{aligned} \quad (2.7)$$

where the ellipses denote terms which do not appear in our calculation. The parameters  $l_i$  and  $h_i$  are the bare LECs and the field strengths are, for our purposes,  $F_L^{\mu\nu} = F_R^{\mu\nu} = Q(\partial^\mu A^\nu - \partial^\nu A^\mu)$ .<sup>6</sup> Note that the  $h_2$  term is a *contact term* and does not contain pion fields.

The lengthy higher-order Lagrangians  $\mathcal{L}_{\text{NNLO}}$  and  $\mathcal{L}_{\text{N}^3\text{LO}}$  are given in refs. [45, 46]. We have implemented the full ChPT lagrangian in **FORM** [43, 44], and the attached code (see sec. G) includes efficient on-the-fly derivation of any Feynman rule from  $\mathcal{L}_{\text{LO}} + \dots + \mathcal{L}_{\text{N}^3\text{LO}}$ .

<sup>5</sup>There is a subtlety here due to the distinct form of the original 2-flavor Lagrangian compared to the later 3- or  $N$ -flavor ones [7]. If done too naively, a reduction from  $N$  to 2 flavors via the Cayley–Hamilton theorem leads to errors in the part of our result where  $\mathcal{L}_4$  enters quadratically (diagrams 10–20 in table 2) due to not fully taking into account the equations of motion remarked in ref. [45].

<sup>6</sup>The Lagrangian is derived under the assumption that  $Q$  (and therefore  $F_{L,R}^{\mu\nu}$ ) is traceless, which is not the case here. However,  $\langle Q^2 \rangle$  and  $\langle Q \rangle^2$  appear here only as  $\langle Q^2 \rangle - \langle Q \rangle^2$ , so the number of degrees of freedom is the same as if  $\langle Q \rangle = 0$ . Therefore, no additional terms are needed in the Lagrangian.

## 2.2 Renormalization

The Lagrangians beyond  $\mathcal{L}_{\text{LO}}$  provide counterterms. At NLO, the renormalization of the LECs in  $d = 4 - 2\epsilon$  dimensions at a scale  $\mu$  (conventionally,  $\mu = 770 \text{ MeV} \approx M_\rho$ ) is

$$l_i = \pi_{16}(c\mu)^{d-4} \left[ l_i^q(\mu) + \frac{\gamma_i}{d-4} \right], \quad h_i = \pi_{16}(c\mu)^{d-4} \left[ h_i^q(\mu) + \frac{\delta_i}{d-4} \right], \quad (2.8)$$

where the  $l_i^q(\mu)$  are the renormalized LECs and  $\pi_{16} := \frac{1}{16\pi^2}$ .<sup>7</sup> We follow ref. [22] in using a convention that more uniformly distributes powers of  $\pi_{16}$ ; the conversion to that of, e.g., refs. [17, 47] is  $l_i^r(\mu) = \pi_{16} l_i^q(\mu)$ . The coefficients  $\gamma_i$  are [6]

$$\gamma_1 = \frac{1}{3}, \quad \gamma_2 = \frac{2}{3}, \quad \gamma_3 = -\frac{1}{2}, \quad \gamma_5 = -\frac{1}{6}, \quad \gamma_6 = -\frac{1}{3}, \quad \gamma_7 = 0, \quad \delta_2 = -\frac{1}{12}. \quad (2.9)$$

The scheme-dependent coefficient  $c$  is conventionally<sup>8</sup>

$$(c\mu)^{d-4} = e^{-\epsilon(\gamma_E + \log \mu^2 - \log 4\pi - 1)} = C(\epsilon, \mu^2) e^\epsilon, \quad (2.10)$$

where  $d = 4 - 2\epsilon$  and  $\gamma_E$  is the Euler–Mascheroni constant. For later convenience, we have defined  $C(\epsilon, z) := e^{-\epsilon(\gamma_E + \log z - \log 4\pi)}$  (see sec. 3).

Similarly, the LECs  $c_i$  of  $\mathcal{L}_{\text{NNLO}}$  are renormalized as

$$c_i = \frac{\pi_{16}^2 (c\mu)^{2(d-4)}}{F_0^2} \left[ c_i^q(\mu) - \frac{\gamma_i^{(2)}}{(d-4)^2} - \frac{\gamma_i^{(1)} + \gamma_i^{(L)}(\mu)}{\pi_{16}(d-4)} \right], \quad (2.11)$$

with coefficients listed in ref. [17]. The  $\gamma_i^{(2)}$  and the  $\gamma_i^{(1)}/\pi_{16}$  are rational numbers like the  $\gamma_i$ , while the  $\gamma_i^{(L)}/\pi_{16}$  are rational linear combinations of the  $l_j^q$ . The factor of  $1/F_0^2$  ensures that the physical LECs are dimensionless.

There currently exists no  $\text{N}^3\text{LO}$  counterpart to ref. [17]. The renormalization of the  $\text{N}^3\text{LO}$  LECs would look analogous to eq. (2.11), including a  $1/(d-4)^3$  term, with all coefficients unknown. However, the  $\text{N}^3\text{LO}$  LECs only appear in very simple terms in our amplitude and need only absorb a limited kind of local divergences. Therefore, the coefficient combinations that appear can simply be inferred from whatever is left after the more involved  $\text{NLO} + \text{NNLO}$  renormalization. We state these expressions in sec. 4.2.

## 2.3 Diagrams

The power-counting scheme of ChPT can be informally stated as follows: for an  $\text{N}^k\text{LO}$  diagram,  $k$  is the order in ChPT’s expansion parameters (not the number of loops). For  $\Pi^{\mu\nu}(q^2)$ , the diagrams at NLO and NNLO are given in table 1, and those at  $\text{N}^3\text{LO}$  in table 2. In particular, note how the lack of vertices with an odd number of pion lines—a consequence of G-parity—strongly limits the available topologies and completely removes the two-loop sunset.

<sup>7</sup>Note that in ref. [17], renormalized quantities are given as functions of  $d$ , which would imply that they possess an  $\epsilon$  expansion whose subleading terms would appear in diagrams containing both counterterms and loops. However, such subleading terms can always be absorbed into the leading part of higher-order LECs, and this is indeed done. (We thank Johan Bijnens for clarifying this point.)

<sup>8</sup>This is the  $\overline{\text{MS}}$  scheme but with  $-1$  added in the exponent, which is the standard scheme for ChPT.

	0	1	2	3	4
0					
1					
1					

**Table 1:** All NLO (top) and NNLO (bottom) diagrams, sorted by ascending number of loops, then roughly by complexity. Unmarked vertices are LO, dots NLO, and squares NNLO. The rows and columns are numbered so that individual diagrams can be easily referenced, such as “14” for the double bubble. The mirror images of the non-symmetric diagrams (03 and 12) are not listed independently. Note that all 2-loop diagrams factor into 1-loop integrals; there are no sunset diagrams.

As is usual with ChPT calculations, the algebraic expressions corresponding to these diagrams are very lengthy, so we used **FORM 4.2** [43, 44] throughout our calculations. To handle the large number of diagrams in a less error-prone way, we used a newly written program that, given a simple description of the diagram topologies, generates the **FORM** code that would in earlier work be written by hand. See sec. G for further information.

## 2.4 Mass and decay constant

The Lagrangian contains the bare pion decay constant,  $F_0$ , and all masses coming from vertices and propagators are nominally the bare pion mass,  $M_0$ . These are related to their renormalized counterparts  $F_\pi$  and  $M_\pi$  (which are scheme-independent physical observables) via

$$M_0^2 \rightarrow M_\pi^2 \left[ 1 + \sum_{i=1}^{\infty} \xi^i \delta M_i \right], \quad F_0 \rightarrow F_\pi \left[ 1 + \sum_{i=1}^{\infty} \xi^i \delta F_i \right], \quad (2.12)$$

where  $\xi := \pi_{16} M_\pi^2 / F_\pi^2$  and the expressions for  $\delta M_i$  and  $\delta F_i$  are given below. An  $N^k$ LO amplitude is then obtained by summing, over  $k' \leq k$ , all contributing  $N^{k'}$ LO amplitudes in which mass and decay constant renormalization has been performed to  $N^{k-k'}$ LO, via the expressions above.

Given the lack of LO diagrams in our case, we only need mass and decay constant renormalization up to NNLO. This was first determined by Bürgi [48], although we use the form given along with the  $N^3$ LO case in ref. [22]:

$$\delta M_i = \sum_{j=0}^i b_{ij}^M L_\pi^j, \quad \delta F_i = \sum_{j=0}^i b_{ij}^F L_\pi^j, \quad (2.13)$$

	0	1	2	3	4
0					
1					
2					
3					
4					
5					
6					
7					
8					
9					
10					

**Table 2:** All N<sup>3</sup>LO diagrams, presented similarly to table 1. Unmarked vertices are LO, dots NLO, squares NNLO, and triangles N<sup>3</sup>LO. The rows and columns are numbered so that individual diagrams can be easily referenced. The mirror images of the non-symmetric diagrams (03, 13, 32–41, etc.) are not listed independently. Note that, unlike at NNLO, there are six 3-loop diagrams (91–101) which do not factor into 1-loop integrals.

where  $L_\pi := \log(M_\pi^2/\mu^2)$  and

$$\begin{aligned}
b_{10}^M &= -2l_3^q, \quad b_{11}^M = -\frac{1}{2}, \quad b_{10}^F = -l_4^q, \quad b_{11}^F = 1, \\
b_{20}^M &= -\frac{163}{96} - 64c_{18}^q - 32c_{17}^q - 96c_{11}^q - 48c_{10}^q + 16c_9^q + 32c_8^q + 16c_7^q + 32c_6^q \\
&\quad - 4l_3^q l_4^q + 8(l_3^q)^2 - 2l_2^q - l_1^q, \\
b_{21}^M &= \frac{13}{3} - l_4^q + 11l_3^q + 8l_2^q + 14l_1^q, \quad b_{22}^M = -\frac{5}{8}, \\
b_{20}^F &= \frac{13}{192} - 8c_9^q - 16c_8^q - 8c_7^q - (l_4^q)^2 + 2l_3^q l_4^q + l_2^q + \frac{1}{2}l_1^q, \\
b_{21}^F &= -\frac{29}{12} + 3l_4^q - 4l_2^q - 7l_1^q, \quad b_{22}^F = -\frac{1}{4}.
\end{aligned} \tag{2.14}$$

### 3 The loop integrals

In this section, we summarize the methods used to reduce and evaluate the loop integrals appearing in  $\Pi^{\mu\nu}(q)$ , unifying the notation relative to the various sources from which they are taken.

#### 3.1 Loop integral manipulations

To write down a family of  $N_L$ -loop integrals with loop momenta  $\{\ell_i\}_{i=1}^{N_L}$  and  $N_p$  independent external momenta  $\{p_i\}_{i=1}^{N_p}$ , one first constructs a set of  $N_k$  momenta  $\{k_j\}_{j=1}^{N_k}$  such that all propagators appearing in the integrals have the form

$$\frac{1}{D_j} := \frac{1}{k_j^2 - m_j^2 + i\epsilon}, \quad j \in \{1, \dots, N_k\}, \tag{3.1}$$

and such that any product  $\ell_i \cdot \ell_j$  or  $\ell_i \cdot p_j$  can be written as a linear combination of inverse propagators  $D_j$  and the masses; this condition fixes  $N_k = N_p N_L + N_L(N_L + 1)/2$ .<sup>9</sup>

In the present case, we only need to consider  $m_j = M_\pi$ . All of the integrals in  $d$  dimensions (which is taken to be an integer minus  $2\epsilon$ ) can be written as

$$[\pi_{16} C(\epsilon, M_\pi^2)]^{N_L} I_{\vec{\nu}}^{(d)}(\{p_i \cdot p_j\}; M_\pi^2) := \int \frac{d^d \ell_1}{\pi^{d/2}} \cdots \int \frac{d^d \ell_{N_L}}{\pi^{d/2}} \prod_{j=1}^{N_k} \frac{1}{D_j^{\nu_j}}, \tag{3.2}$$

where  $\vec{\nu} \in \mathbb{Z}^{N_k}$  is a vector of integers that distinguishes members of the integral family. This accommodates integrals with nontrivial numerators as long as they consist only of scalar products, since these can be accounted for with negative  $\nu_j$ . The Wick rotation to Euclidean space takes the form  $I_{\vec{\nu}} \rightarrow i^{N_L} (-1)^{\sum_j \nu_j} I_{\vec{\nu}}^E$ .

Note in eq. (3.2) how we use the same normalization factor  $C(\epsilon, M_\pi^2)$  as in eq. (2.10), albeit with  $M_\pi^2$  instead of  $\mu^2$ ; this simplifies dimensional regularization and also ensures that  $I_{\vec{\nu}}^{(d)}$  has integer mass dimension. After the conversion  $C(\epsilon, \mu^2) = C(\epsilon, M_\pi^2) e^{\epsilon L}$ , all

<sup>9</sup>To see that the number of distinct propagators never exceeds this  $N_k$ , consider a connected graph with  $N_V$  vertices,  $N_E$  internal edges and  $N_L$  loops, ignoring 2-point vertices since these do not affect the number of distinct propagators. Thus, each vertex has at least 3 legs, each of which is either an external leg or half an edge, so that  $N_p + 2N_E \geq 3N_V$ . Combining this with Euler's formula,  $N_V - N_E + N_L = 1$ , yields  $N_E \leq 3(N_L + 1) + N_p$ , which implies  $N_E < N_k$  for all  $N_L \geq 1, N_p \geq 0$ .

diagrams at  $N^k$ LO will, when expressed in terms of  $I_{\bar{\nu}}$  and renormalized LECs, contain  $C(\epsilon, M_\pi^2)^k$ , which can be kept as-is throughout the calculations until the  $\epsilon \rightarrow 0$  limit can be safely taken with  $C(0, M_\pi^2) = 1$ . The  $\pi_{16}(4\pi)^\epsilon$  contained in the normalization of  $I_{\bar{\nu}}$  compensates for how we normalize with  $\pi^{d/2}$  in eq. (3.2) (which simplifies many formulae below) rather than  $(2\pi)^d$  (which is how the integrals appear in the diagrams).

There exist a large number of techniques for manipulating loop integrals, and in sec. A we provide some details on those used in this work. In summary, we first use integration-by-parts relations to express all integrals in terms of a small number of *master integrals* listed below. All subsequent calculation efforts can then be concentrated on these. Tarasov's dimensional shift [23] is then used to relate master integrals in  $d$  dimensions to those in  $d-2$ , simplifying renormalization since lower-dimensional integrals are typically less divergent. We also derive novel Schouten relations which, in the vicinity of integer dimension, provide additional relations between the master integrals. Lastly, we derive differential equations satisfied by the integrals, allowing them to be computed without explicitly integrating any loop momenta.

There exist several excellent programs for performing the reduction to master integrals, but in this work we exclusively use `LiteRed 2` [49, 50],<sup>10</sup> along with `pySecDec` [51–54] for numerically verifying the various integral manipulations.

### 3.2 Master integrals of $\Pi^{\mu\nu}(q^2)$ at three-loop order

We use the following basis, which allows writing all three-loop integrals appearing in  $\Pi^{\mu\nu}(q)$ :

$$\{k_j\}_{j=1}^9 = \{\ell_1, \ell_2, \ell_3, \ell_1 - q, \ell_2 - q, \ell_3 - q, \ell_1 + \ell_3, \ell_2 + \ell_3, \ell_1 + \ell_2\}. \quad (3.3)$$

For 2-loop integrals, we use the subset  $\{k_1, k_2, k_4, k_5, k_9\}$ , and for 1-loop integrals,  $\{k_1, k_4\}$ . In order to simplify our expressions, we write the master integrals as functions of the dimensionless parameter  $t := q^2/M_\pi^2$ , suppress their dependence on  $M_\pi$ , and render all master integrals dimensionless at  $d = 2$  with an appropriate power of  $M_\pi$ .

At one-loop order, the set of master integrals is simply the tadpole ( $\mathcal{Q}$ ) and bubble ( $\mathcal{O}$ ):

$$I_{1,0}^{(d)}(q^2, M_\pi) =: I_{\mathcal{Q}}(d), \quad M_\pi^2 I_{1,1}^{(d)}(q^2, M_\pi) =: I_{\mathcal{O}}(d; t). \quad (3.4)$$

Thanks to our choice of  $C(\epsilon, M_\pi^2)$ , the expression for the former is exceedingly simple:

$$I_{\mathcal{Q}}(4 - 2\epsilon) = -i\Gamma(\epsilon - 1) = \frac{i \exp \left[ \sum_{k=2}^{\infty} (-\epsilon)^k \frac{\zeta(k)}{k} \right]}{\epsilon(1 - \epsilon)}, \quad (3.5)$$

using the relation between  $\log \Gamma(z)$  and the Riemann zeta function  $\zeta(z) = \sum_{n=1}^{\infty} n^{-z}$ . The latter is similar, and textbook manipulations put it in the form

$$I_{\mathcal{O}}(4 - 2\epsilon; t) = (1 - \epsilon) I_{\mathcal{Q}}(4 - 2\epsilon) \int_0^1 \frac{dx}{[1 - x(1 - x)t]^\epsilon}, \quad (3.6)$$

---

<sup>10</sup>We have unsuccessfully tried to perform the reduction also in other programs, but have been hampered by crashes or extremely long running times. Out of the box, `LiteRed 2` requires  $\mathcal{O}(1 \text{ hour})$  to determine the general reduction rules for our propagators, which needs to be done only once, and can then reduce all integrals in  $\Pi^{\mu\nu}(q)$  in  $\mathcal{O}(1 \text{ minute})$ .

where we write the Feynman parameter integral as<sup>11</sup>

$$\int_0^1 \frac{dx}{[1-x(1-x)t]^\epsilon} = 1 + \sum_{n=1}^{\infty} (-\epsilon)^n \frac{J_{\circlearrowleft}^{(n)}(t)}{n!}, \quad J_{\circlearrowleft}^{(n)}(t) := \int_0^1 dx \log^n [1-x(1-x)t] \quad (3.7)$$

and express our results in terms of  $J_{\circlearrowleft}^{(n)}(t)$ , which are given explicitly in sec. D.1.

We have three two-loop master integrals, but as remarked in table 1, these simply factorize into tadpoles and bubbles. Adopting the tadpole-bubble product notation

$$T_{ab}(d; t) := [I_{\circlearrowleft}(d)]^a [I_{\circlearrowright}(d; t)]^b, \quad (3.8)$$

they are

$$\begin{aligned} I_{1,1,0,0,0}^{(d)}(q^2, M_\pi) &= T_{20}(d), & M_\pi^2 I_{1,1,1,0,0}^{(d)}(q^2, M_\pi) &= T_{11}(d; t), \\ M_\pi^4 I_{1,1,1,1,0}^{(d)}(q^2, M_\pi) &= T_{02}(d; t). \end{aligned} \quad (3.9)$$

At three loops, we have 11 master integrals. Of these, four are again factorizable into tadpole-bubble products:

$$\begin{aligned} I_{1,1,1,0,0,0,0,0,0}^{(d)}(q^2, M_\pi) &= T_{30}(d), & M_\pi^4 I_{1,1,1,1,1,0,0,0,0}^{(d)}(q^2, M_\pi) &= T_{12}(d; t), \\ M_\pi^2 I_{1,1,1,1,0,0,0,0,0}^{(d)}(q^2, M_\pi) &= T_{21}(d; t), & M_\pi^6 I_{1,1,1,1,1,1,0,0,0}^{(d)}(q^2, M_\pi) &= T_{03}(d; t). \end{aligned} \quad (3.10)$$

The remaining ones are highly nontrivial, and we name them as follows:<sup>12</sup>

$$\begin{aligned} M_\pi^2 I_{1,1,0,0,0,0,1,1,0}^{(d)}(q^2, M_\pi) &=: E_0(d), & M_\pi^4 I_{1,1,0,1,0,0,1,1,0}^{(d)}(q^2, M_\pi) &=: E_4(d; t), \\ M_\pi^2 I_{1,0,0,0,1,0,1,1,0}^{(d)}(q^2, M_\pi) &=: E_1(d; t), & M_\pi^6 I_{1,1,0,1,1,0,1,1,0}^{(d)}(q^2, M_\pi) &=: E_5(d; t), \\ M_\pi^4 I_{2,0,0,0,1,0,1,1,0}^{(d)}(q^2, M_\pi) &=: E_2(d; t), & M_\pi^8 I_{2,1,0,1,1,0,1,1,0}^{(d)}(q^2, M_\pi) &=: E_6(d; t), \\ M_\pi^6 I_{3,0,0,0,1,0,1,1,0}^{(d)}(q^2, M_\pi) &=: E_3(d; t), \end{aligned} \quad (3.11)$$

where ‘‘E’’ refers to the fact that their evaluation involves elliptic integrals (see sec. E). The vacuum integral  $E_0(d)$  is simply  $E_1(d; 0)$ , and  $E_2$  and  $E_3$  can be related to the first and second  $t$ -derivatives of  $E_1$  (see sec. B); likewise,  $E_6$  is related to the derivative of  $E_5$ . The general layout of the integrals is illustrated in fig. 1.

All  $E_i$  are divergent in four dimensions but finite in two, so we employ Tarasov’s dimensional shift to extract their divergences. Going forward, we use the following notation for the master integrals as series in  $\epsilon$ :

$$E_i(4 - 2\epsilon; t) = \sum_{r=-3}^{\infty} \epsilon^r E_i^{(r)}(4; t), \quad E_i(2 - 2\epsilon; t) = \sum_{r=0}^{\infty} \epsilon^r E_i^{(r)}(2; t). \quad (3.12)$$

Since the integrals are finite in two dimensions, we simply have  $E_i(2; t) = E_i^{(0)}(2; t)$ , whereas we refer to the finite part in four dimensions as  $\bar{E}_i(4; t) := E_i^{(0)}(4; t)$ .

<sup>11</sup>The notation is inspired by the standard bubble function  $\bar{J}(M_\pi^2, q^2) = -\pi_{16} J_{\circlearrowleft}^{(1)}(t)$ .

<sup>12</sup>For comparison, ref. [22] has two such non-factorizable three-loop master integrals (plus one at two loops, namely the sunset  $I_{1,0,0,1,1}$ ). In our notation, they are  $E_0$  and  $I_{1,1,0,0,0,1,1,1,0}$ , the latter of which does not appear in our set. Both are known from earlier gauge theory calculations [55].

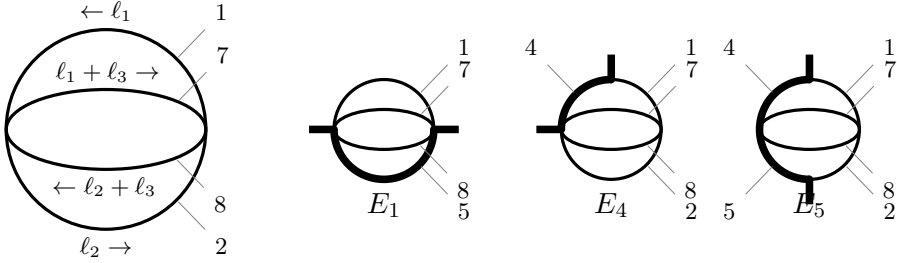


**Figure 1:** From left to right: the basic topology and momentum routing common to all  $E_i$  integrals, corresponding in that form to the vacuum integral  $E_0$ ; the same with an external momentum  $q$  routed through the thicker line, giving  $E_1$ ; ditto for  $E_4$ ; ditto for  $E_5$ . Each line is tagged with its index  $i$ : it carries momentum  $k_i$  given in eq. (3.3) and occurs with power  $\nu_i$  in  $I_{\vec{\nu}}$ .

## 4 Results

In this section, we present our main result, namely  $\Pi_T(q^2)$  [i.e., the transverse component of  $\Pi^{\mu\nu}(q^2)$  as defined in eqs. (2.1) and (2.3)], computed to N<sup>3</sup>LO as outlined in previous sections. Besides being a function of the pion mass  $M_\pi^2$ , the pion decay constant  $F_\pi^2$  and the photon momentum  $q^\mu$  through  $t := q^2/M_\pi^2$ , it also contains the renormalized low-energy constants  $l_i^q$  and  $c_i^q$ , as well as  $r_i^q$ , which are defined below in sec. 4.2. These are all functions of the renormalization scale  $\mu$  in the customary ChPT renormalization scheme, while  $\Pi_T$  itself is kept scale-independent through the appearance of  $L_\pi := \log \frac{M_\pi^2}{\mu^2}$ , which in turn emerges from the mass and decay constant renormalization, and from reconciling the factors of  $C(\epsilon, \mu^2)$  in the LECs with those of  $C(\epsilon, M_\pi^2)$  in the loop integrals (see sec. 3.1). The constant  $\zeta(3) = 1.202\dots$  also appears.

The  $t$ -dependence of the result is expressed using the functions  $J_{\circlearrowleft}^{(n)}(t)$  defined in eq. (3.7) and evaluated in sec. D.1;  $E_1(2; t)$ ,  $E_2(2; t)$  and  $E_3(2; t)$  defined in eq. (3.11), shifted to 2 dimensions using the method described in sec. A.2 and evaluated in sec. E;  $\bar{E}_5(4; t)$  and  $\bar{E}_6(4; t)$  defined in eq. (3.12) and evaluated in sec. D. The reason for using a mix of 2- and 4-dimensional integrals was explained in sec. A.3.

We have subjected the result to the following checks:

- The longitudinal part  $\Pi_L(q^2)$  vanishes, as required by the Ward–Takahashi identity;
- All non-local divergences are removed by the renormalization, and the local ones are of a form that allows them to be canceled by the N<sup>3</sup>LO counterterms (see sec. 4.2);
- The result is invariant under reparametrization of the Nambu–Goldstone manifold, e.g., replacing eq. (2.5) by  $U = e^{i\Phi/F_0\sqrt{2}}$ , or more generally following ref. [56, app. B];
- There are no singularities at  $t = 0$  despite the presence of factors of  $\frac{1}{t}$ ;<sup>13</sup>

<sup>13</sup>That such factors appear can be viewed as a consequence of our choice of master integrals (and  $J_{\circlearrowleft}^{(n)}$ ). While a choice that absorbs them would certainly be possible—compare the use of  $\bar{B}_{21}$  rather than the scalar bubble integral in ref. [40]—we have found it simpler to retain the “natural” master integrals, at the cost of having to take the  $t \rightarrow 0$  limit more carefully.

- The above checks hold also when the calculation is repeated at 3 or  $N$  mass-degenerate flavors, to ensure that no errors have been made whose effects just happen to vanish in the 2-flavor case;
- Restricting the calculation to NLO or NNLO reproduces earlier results [6, 7, 40–42]; see eqs. (4.2) and (4.3).

#### 4.1 Expressions for the HVP

As discussed above, the longitudinal component,  $\Pi_L(q^2)$ , vanishes identically, so we only consider the transverse component  $\Pi_T(q^2)$ , which we renormalize on shell, as done in most physical applications. Thus, we present results for  $\bar{\Pi}_T(q^2) := \Pi_T(q^2) - \Pi_T(0)$ , deferring discussion of the unsubtracted quantity  $\Pi_T(q^2)$  to sec. F. We expand the result in powers of  $\xi$ ,

$$\frac{1}{\pi_{16}}\bar{\Pi}_T(q^2) = \bar{\Pi}_T^{\text{NLO}}(t) + \xi\bar{\Pi}_T^{\text{NNLO}}(t) + \xi^2\bar{\Pi}_T^{\text{N}^3\text{LO}}(t) + \mathcal{O}(\xi^3), \quad (4.1)$$

where, as in sec. 2.4,  $\xi := \pi_{16}M_\pi^2/F_\pi^2 \approx 0.03$  and  $\pi_{16} := \frac{1}{16\pi^2}$ . Note that on the right-hand side, we deliberately write the  $\bar{\Pi}$ 's as dimensionless functions of  $t$ .

The first two terms in eq. (4.1) are known from earlier work [6, 7, 40–42], but we restate them here in our notation:<sup>14</sup>

$$\bar{\Pi}_T^{\text{NLO}}(t) = 2\frac{4-t}{3t}J_{\text{--}}^{(1)}(t) + \frac{4}{9}, \quad (4.2)$$

$$\bar{\Pi}_T^{\text{NNLO}}(t) = t\left[\frac{4-t}{3t}J_{\text{--}}^{(1)}(t) - \frac{1+3L_\pi}{9}\right]^2 - 4t\left[\frac{4-t}{3t}J_{\text{--}}^{(1)}(t) - \frac{1+3L_\pi}{9}\right]l_6^q - 8tc_{56}^q. \quad (4.3)$$

The novel third term is much lengthier, so for the sake of presentation we partition it thematically,<sup>15</sup>

$$\bar{\Pi}_T^{\text{N}^3\text{LO}}(t) = \bar{\Pi}_E(t) + \bar{\Pi}_J(t) + \bar{\Pi}_\zeta(t) + \bar{\Pi}_l(t) + \bar{\Pi}_c(t) + tr_1^q + t^2r_2^q, \quad (4.4)$$

where the  $\text{N}^3\text{LO}$  LECs  $r_i^q$  come from the contact diagram 00 in table 2 and are discussed

<sup>14</sup>Refs. [40–42] express the non-polynomial  $t$ -dependence in terms of the functions  $\bar{B}_{21}$  and  $\bar{B}_{22}$ , which derive from the finite part of the rank-2 tensor bubble integral. Here, “finite part” is defined by writing the divergence in terms of  $\lambda_0 = [1 + \frac{1}{\epsilon}]C(\epsilon, M_\pi^2) + \mathcal{O}(\epsilon)$ . The relation to our conventions is thus

$$\bar{B}_{21}(M_\pi^2, M_\pi^2, q^2) = \pi_{16}\left(\frac{1-t}{3t}J_{\text{--}}^{(1)}(t) + \frac{1}{3}L_\pi - \frac{5}{18}\right), \quad \bar{B}_{22}(M_\pi^2, M_\pi^2, q^2) = \pi_{16}\left(\frac{t-4}{12}J_{\text{--}}^{(1)}(t) + \frac{t-6}{12}L_\pi + \frac{t}{36}\right).$$

<sup>15</sup>While there is significant mixing due to master integral reduction and renormalization,  $\bar{\Pi}_c$  can be said to mainly stem from diagrams 01–04 in table 2,  $\bar{\Pi}_l$  from 10–53,  $\bar{\Pi}_J$  from 54–90, and  $\bar{\Pi}_E$  from 91–101.

further in sec. 4.2. The part containing the elliptic master integrals  $E_i$  is

$$\begin{aligned}\bar{\Pi}_E(t) = & \left[ \frac{107t^3}{46656} - \frac{233t^2}{3888} - \frac{47t}{243} + \frac{17327}{1458} - \frac{20813}{486t} + \frac{1952}{81t^2} \right] E_1(2; t) \\ & - \left[ \frac{143t^4}{46656} - \frac{257t^3}{1944} + \frac{2209t^2}{1944} + \frac{32287t}{2916} - \frac{32126}{243} + \frac{72214}{243t} - \frac{7808}{81t^2} \right] E_2(2; t) \\ & - \left[ \frac{143t^4}{23328} - \frac{166t^3}{729} + \frac{316t^2}{243} + \frac{29413t}{1458} - \frac{99722}{729} + \frac{5216}{27t} \right] E_3(2; t) \\ & - \left[ \frac{t}{3} - \frac{13}{9} - \frac{2}{3t} \right] \bar{E}_5(4; t) + \left[ \frac{t^3}{54} - \frac{19t^2}{27} + \frac{143t}{27} - \frac{100}{9} \right] \bar{E}_6(4; t),\end{aligned}\quad (4.5)$$

the part containing the bubble functions  $J_{\circlearrowleft}^{(n)}$  (but no LECs) is

$$\begin{aligned}\bar{\Pi}_J(t) = & - \left[ \frac{t^2}{648} + \frac{t}{324} - \frac{1}{108} - \frac{1}{9t} \right] J_{\circlearrowleft}^{(3)}(t) - \left[ \frac{t^2}{54} - \frac{8t}{27} + \frac{4}{3} - \frac{2}{3t} \right] J_{\circlearrowleft}^{(2)}(t) J_{\circlearrowleft}^{(1)}(t) \\ & - \left[ \frac{t^2}{54} - \frac{2t}{9} + \frac{8}{9} - \frac{32}{27t} \right] [J_{\circlearrowleft}^{(1)}(t)]^3 - \left[ \frac{5t^2}{216} - \frac{103t}{108} + \frac{151}{36} + \frac{1}{3t} \right] J_{\circlearrowleft}^{(2)}(t) \\ & - \left[ \frac{(1+L_\pi)t^2}{27} - \frac{(63+4L_\pi)t}{54} + \frac{275-64L_\pi}{54} + \frac{10+96L_\pi}{27t} \right] [J_{\circlearrowleft}^{(1)}(t)]^2 \\ & + \left[ \frac{(97-9\pi^2)t^2}{3888} - \frac{(2285+9\pi^2)t}{1944} + \frac{407}{81} + \frac{\pi^2}{72} - \frac{4-\pi^2}{6t} \right] J_{\circlearrowleft}^{(1)}(t) \\ & - \left[ \frac{t^2 L_\pi}{27} + \frac{(23+8L_\pi)t}{27} - \frac{92+48L_\pi}{27} \right] L_\pi J_{\circlearrowleft}^{(1)}(t)\end{aligned}\quad (4.6)$$

the part containing neither  $E_i$ ,  $J_{\circlearrowleft}^{(n)}$  nor LECs is

$$\begin{aligned}\bar{\Pi}_\zeta(t) = & - \frac{48t^2 - 7957t - 96}{432t} \zeta(3) - \frac{t^2 + 18t}{81} L_\pi^3 - \frac{20t}{27} L_\pi^2 - \left[ \frac{17t^2}{432} - \frac{845t}{648} \right] L_\pi \\ & - \left[ \frac{t^2}{216} - \frac{5t}{27} + \frac{22}{27} + \frac{1}{18t} \right] \pi^2 + \frac{20245t^2}{139968} - \frac{55511t}{23328} - \frac{52285}{1944} + \frac{1216}{27t},\end{aligned}\quad (4.7)$$

the NLO LEC part is

$$\begin{aligned}\bar{\Pi}_l(t) = & t \left[ \frac{4-t}{3t} J_{\circlearrowleft}^{(1)}(t) - \frac{1+3L_\pi}{9} \right]^2 \left( [l_2^q - 2l_1^q - 2l_6^q]t + 2l_4^q \right) + 4L_\pi [l_6^q]^2 \\ & - 2t \left[ \frac{4-t}{3t} J_{\circlearrowleft}^{(1)}(t) - \frac{1+3L_\pi}{9} \right] \left( 2L_\pi [2l_1^q - l_2^q - 2l_6^q] - l_6^q [4l_4^q - tl_6^q] \right),\end{aligned}\quad (4.8)$$

and, lastly, the NNLO LEC part is

$$\begin{aligned}\bar{\Pi}_c(t) = & 4 \left[ \frac{4-t}{3} J_{\circlearrowleft}^{(1)}(t) - t \frac{1+3L_\pi}{9} \right] (r_{V1}^q + tr_{V2}^q) \\ & + 8L_\pi (r_{V2}^q - 4tc_{50}^q) + 16t(L_\pi - l_4^q)c_{56}^q,\end{aligned}\quad (4.9)$$

where  $r_{V1}^q := -4(2c_{53}^q + 2c_{35}^q + 4c_6^q)$  and  $r_{V2}^q := 4(c_{53}^q - c_{51}^q)$  are the combinations of NNLO LECs appearing in the  $\mathcal{O}(t)$  and  $\mathcal{O}(t^2)$  terms, respectively, of the small- $t$  expansion of the pion vector form-factor  $F_V^\pi(t)$  [21]; these are discussed further in sec. 4.3.

Eqs. (4.5) to (4.9) comprise, via eq. (4.4), the main result of this work.

## 4.2 N<sup>3</sup>LO renormalization

Unlike at lower order [6, 17], the explicit renormalization of the N<sup>3</sup>LO LECs has not been worked out in the literature. However, these LECs only enter through the contact diagram 00 in table 2, which evaluates to a quadratic polynomial in  $t$ :

$$\text{~~~~~} \Delta \text{~~~~~} = r_0 + tr_1 + t^2 r_2. \quad (4.10)$$

With  $\tilde{c}_n$  the LEC of term  $n$  in the 2-flavor N<sup>3</sup>LO Lagrangian [46], the coefficients  $r_i$  are

$$\begin{aligned} -r_0 &= 64(\tilde{c}_{382} + \tilde{c}_{383}) + 4\tilde{c}_{457} + 8(\tilde{c}_{458} + \tilde{c}_{474}) + 16\tilde{c}_{475}, \\ r_1 &= 16(\tilde{c}_{332} - \tilde{c}_{333}), \quad r_2 = -8\tilde{c}_{459}, \end{aligned} \quad (4.11)$$

which we symbolically renormalize via [compare eqs. (2.8) and (2.11)]

$$r_i = \pi_{16}^3 (c\mu)^{3(d-4)} \left[ r_i^q(\mu) + \sum_{j=1}^3 \frac{\gamma_{ij}}{(d-4)^j} \right]. \quad (4.12)$$

The leading divergence of the sum of diagrams 01–101 in table 2 is  $\frac{8t^2}{81\epsilon^3}$ , so we must have  $\gamma_{03} = \gamma_{13} = 0$  and  $\gamma_{23} = -\frac{8}{81}$  in order to cancel this divergence.<sup>16</sup> Likewise, from the subleading divergences we deduce

$$\begin{aligned} \gamma_{01} &= -\frac{208}{27} - \frac{16}{3}l_2^q - \frac{8}{3}l_1^q - 32l_3^ql_6^q + 64l_3^ql_5^q - 64c_{50}^q + 256c_{47}^q - 128c_{46}^q + 64c_{44}^q \\ &\quad - 64c_{35}^q + 224c_{34}^q + 16c_{33}^q - 24c_{32}^q - 24c_{31}^q + 32c_{30}^q - 96c_{29}^q - 384c_6^q, \\ \gamma_{02} &= -\frac{184}{9} - 16l_6^q + 32l_5^q - 16l_2^q + 32l_1^q, \\ \gamma_{11} &= \frac{1013}{972} + 8(l_6^q)^2 + \frac{256}{3}c_{53}^q - 64c_{51}^q - 64c_{50}^q + \frac{32}{3}c_{35}^q + \frac{128}{3}c_6^q, \\ \gamma_{12} &= \frac{128}{81} + \frac{16}{3}l_2^q - \frac{32}{3}l_1^q, \\ \gamma_{21} &= -\frac{169}{5832} - \frac{4}{3}(l_6^q)^2 - \frac{32}{3}c_{53}^q + \frac{32}{3}c_{51}^q, \\ \gamma_{22} &= -\frac{8}{243} + \frac{8}{9}l_6^q - \frac{4}{9}l_2^q + \frac{8}{9}l_1^q. \end{aligned}$$

This makes our result finite.

## 4.3 Dependence on the LECs

The values of the NLO LECs appearing in our result are [47]<sup>17</sup>

$$l_1^q = -0.65 \pm 0.10, \quad l_2^q = 0.273 \pm 0.033, \quad l_4^q = 0.92 \pm 0.20, \quad l_6^q = -1.96 \pm 0.07. \quad (4.13)$$

However, as can be seen in eq. (4.8),  $l_1^q$  and  $l_2^q$  only appear in the combinations

$$(l_2^q - 2l_1^q - 2l_6^q) = 5.9 \pm 0.4, \quad (2l_1^q - l_2^q - 2l_6^q) = 2.8 \pm 0.4. \quad (4.14)$$

<sup>16</sup>Since  $r_2$  only contains one LEC, the contact term  $\tilde{c}_{459}(\langle D^2 F_L^{\mu\nu} D^2 F_{L\mu\nu} \rangle + \langle D^2 F_R^{\mu\nu} D^2 F_{R\mu\nu} \rangle)$  is being the first (and, at the time of writing, only) term in the N<sup>3</sup>LO Lagrangian [46] to be explicitly renormalized.

<sup>17</sup>As can be seen in sec. F, also  $l_5^q = -0.730 \pm 0.018$  appears in  $\Pi_T(q^2)$ . Note that refs. [21, 47, etc.] use the “ $r$ ” normalization convention:  $l_i^r = \pi_{16} l_i^q$  (recall sec. 2.2).

While all NLO LECs are known to some precision, the NNLO LECs are generally not. Fortunately,  $r_{V2}^q$  [recall eq. (4.9)] is among the few accurately measured ones [47], and also  $r_{V1}^q$  can be determined from measurements of the pion charge radius [57, 58], although it is dominated by uncertainties in the NLO contributions and therefore not very accurate:<sup>18</sup>

$$r_{V1}^q = -5 \pm 8, \quad r_{V2}^q = 4.0 \pm 1.2. \quad (4.15)$$

Compare the estimate  $r_{V1}^q \approx -6.2$  from vector meson dominance [21].

Two more linear combinations of NNLO LECs appear in the last line of eq. (4.9), but they are of lesser importance, since they lack  $J_{\circlearrowleft}^{(1)}(t)$  and therefore do not contribute to the imaginary part, and since they combine with the entirely undetermined N<sup>3</sup>LO LEC  $r_1^q$ . However, in the computation of FVEs only terms associated with loops survive. In the last line of eq. (4.9), these are  $-32tL_\pi c_{50}^q$  (from diagram 01 in table 2) and  $16tL_\pi c_{56}^q$  (via a tadpole loop in the decay constant renormalization), so for FVEs only the combination  $2c_{50}^q - c_{56}^q$  is needed. These LECs appear in different linear combinations at two loops in the vector-vector and axial-axial correlators (with  $c_{50}, c_{56}$  appearing as  $C_{87}, C_{93}$  at three flavors [41] and as  $K_{109}, K_{115}$  at  $n$  flavors [42]), so their values can be determined if needed.

## 5 Conclusions and outlook

We have computed the three-loop HVP amplitude  $\Pi^{\mu\nu}(q)$  in two-flavor ChPT. We have given the result in terms of three (poly)logarithmic and five elliptic functions of the photon virtuality, with four of the elliptic functions being new to this work. While the polynomial part of the amplitude depends on entirely unknown LECs, the (poly)logarithmic part depends on only five parameters, all more or less known from data, and the elliptic part has no free parameters. Our result provides the next-to-next-to-leading contribution to the subthreshold part of the amplitude and its two-pion cut, and the leading contribution to the four-pion cut, which comes entirely from the elliptic part.

The process of evaluating the amplitude has required unexpectedly deep forays into the field of loop integrals. Satisfying the Ward–Takahashi identity required state-of-the-art master integral reduction, and renormalization required a step beyond that with the novel Schouten relations. While relatively accessible methods allowed all our elliptic integrals to be related to a single one,  $E_1$ , which is well-studied and amenable to powerful mathematical approaches, the sheer complexity of putting this to use has prompted us to split off the numerical implementation into a follow-up work [39] in order to keep the present scope manageable. As it stands, the amplitude can be evaluated using `pySecDec` [51–54], although the precision is very limited for many virtualities, particularly above threshold.

The HVP amplitude, in particular when completed in ref. [39], serves as a starting point for the wide range of phenomenological applications surveyed in the introduction. Not least among these are FVEs, and even if the most direct approach then is to recompute

---

<sup>18</sup>Again, note the normalization convention:  $r_{Vi}^r = \pi_{16}^2 r_{Vi}^q$ . Since the publication of the LEC values used here, there has been significant progress in the measurement of the observables from which they are determined (see, e.g., ref. [59] for the pion charge radius). Thus, it should be possible to improve the precision of  $r_{Vi}^q$ .

the amplitude in a finite volume, this completed infinite-volume calculation can serve as a blueprint for that undertaking. This work also leaves us in a better position to consider if there are other three-loop ChPT calculations that may prove both useful and tractable.

### Acknowledgements

We would like to thank Antonin Portelli for invaluable discussions about the finite-volume HVP at three loops, toward which we hope that the present calculation is a big step on the way. We would also like to thank Roman Lee and Lorenzo Trancredi for very useful discussions regarding the integrals, and Johan Bijnens and Marc Knecht regarding ChPT. MS would particularly like to thank Johan Bijnens for the use of his `FORM` codes, which were an invaluable reference in the development of the `FORM` code used here.

The work of PV was funded by the Agence Nationale de la Recherche (ANR) under the grant Observables (ANR-24-CE31-7996), and by the Munich Institute for Astro-, Particle and BioPhysics (MIAPbP) which is funded by the Deutsche Forschungsgemeinschaft (DFG, German Research Foundation) under Germany’s Excellence Strategy – EXC-2094 – 390783311. The work of LL, AL and MS was funded by the French government under the France 2030 investment plan, as part of the “Initiative d’Excellence d’Aix-Marseille Université – A\*MIDEX” under grant AMX-22-RE-AB-052, and by the ANR under grant ANR-22-CE31-0011.

## A More on loop integral manipulations

We apply various techniques to reduce the number of loop integrals and to compute them, some rather standard and others less so. While the explicit expressions resulting from these techniques are lengthy enough that we defer them to their own appendices, this appendix is intended to provide an overview. We use the notation of sec. 3 throughout, and abbreviate eq. (3.2) as  $I_{\vec{\nu}} = \int J_{\vec{\nu}}$ .

The common theme of these techniques is the application of differential operators to the integrands (see, e.g., refs. [60, 61] for expository texts). Perhaps the most familiar example is integration by parts (IBP), namely the identity

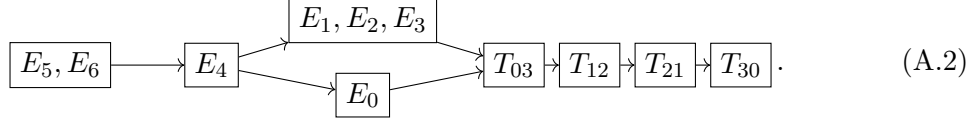
$$0 = \int \frac{\partial}{\partial \ell_i^\mu} (r^\mu J_{\vec{\nu}}) , \quad (\text{A.1})$$

where  $\ell_i$  is any of the loop momenta and  $r$  is any momentum, loop or external. Evaluating the derivative gives a linear combination of integrands  $J_{\vec{\nu}'}$  for various  $\vec{\nu}'$ , so each choice of  $(\vec{\nu}, \ell_i, r)$  gives a linear combination of integrals  $I_{\vec{\nu}'}$  that is known to vanish. The resulting system of equations can be solved systematically using the Laporta algorithm [62], of which programs such as `LiteRed` [49, 50] are essentially implementations with various heuristic improvements. Thus, any Feynman integral  $I_{\vec{\nu}}$ ,  $\vec{\nu} \in \mathbb{Z}^{N_k}$  can be expressed in terms of a *finite* basis of master integrals [63–65].

### A.1 Differential equations

A useful property of derivatives with respect to masses and momenta is that they can only change the power to which an existing propagator appears in the integrand, but never make

a new propagator appear. This produces a hierarchy among the master integrals based on the propagators they contain, which in our three-loop case looks schematically like



Here,  $[A] \rightarrow [B]$  means that the set of propagators in  $B$  is a subset of those of  $A$ , and we say that  $B$  is lower in the hierarchy. Applying a differential operator to a master integral gives, after reduction, a linear combination of master integrals at the same level or lower in the hierarchy as the original integral, never higher.

A salient case is  $\partial/\partial t$ , or in general the derivative with respect to any kinematical invariant. Say that  $\{\mathcal{M}_i\}_{i=1}^n$  are the master integrals living on some level in the hierarchy. Then, schematically,

$$\frac{\partial}{\partial t} \mathcal{M}_i(d; t) = \sum_{j=1}^n \rho_{ij}(d; t) \mathcal{M}_j(d; t) + \mathcal{S}_i(d; t), \quad (\text{A.3})$$

where  $\rho_{ij}$  are rational functions and  $\mathcal{S}_i$  contains only integrals lower in the hierarchy. Taking further derivatives produces the same general structure as eq. (A.3), yielding a system of relations that allow the other  $\mathcal{M}_j$ ,  $j \neq i$  to be traded for derivatives of  $\mathcal{M}_i$ . Solving the system to eliminate the other  $\mathcal{M}_j$  gives the inhomogeneous differential equation

$$\sum_{j=0}^n \pi_{ij}(d; t) \left[ \frac{\partial}{\partial t} \right]^j \mathcal{M}_i(d; t) = \mathcal{S}'_i(d; t), \quad (\text{A.4})$$

where  $\pi_{ij}(d; t)$  are polynomials, and the inhomogeneous part  $\mathcal{S}'_i$  consists of integrals lower in the hierarchy.

Solving such a differential equation (with the simpler integral obtained at  $t = 0$  as initial condition) is a viable alternative to direct integration [see, e.g., ref. [32, 34, 35], which yield  $E_1(2; t)$ ]. We list these equations (with  $n = 3$  for  $E_1, E_2, E_3$ ,  $n = 2$  for  $E_5, E_6$ , and  $n = 1$  for  $E_4$ ) in sec. B. The method outlined here is a simple way of obtaining differential equations satisfied by the master integrals in general dimensions [33]. In fixed dimensions one needs to resort to the Picard-Fuchs algorithm [36, 37]. This algorithm also gives a direct way of deriving the differential equations satisfied by a given Feynman integral without requiring an explicit master integral reduction.

## A.2 Tarasov's dimensional shift

A more straightforward differential operator is  $\partial/\partial m_i^2$ , if we treat all propagators as having distinct masses; the equal-mass limit can be taken after it has been applied. It acts as

$$\frac{\partial}{\partial m_i^2} \frac{1}{D_j^\nu} = \frac{\nu \delta_{ij}}{D_j^{\nu+1}} \quad \Rightarrow \quad \frac{\partial}{\partial m_i^2} I_{\vec{\nu}} = \nu_i I_{\vec{\nu}+\hat{i}}, \quad (\text{A.5})$$

where the  $i$ th component of  $\hat{i}$  is 1 and the others 0.

Following a trick due to Tarasov [23], this operator is utilized to formally change the dimension of an integral in steps of 2. The formula is best introduced by first bringing the integrals to parametric form by using the identity

$$\Gamma(\nu) := \int_0^\infty d\alpha \alpha^{\nu-1} e^{-\alpha} = D^\nu \int_0^\infty d\alpha \alpha^{\nu-1} e^{-\alpha D}, \quad (\text{A.6})$$

where in the second equality we shifted  $\alpha \rightarrow \alpha D$ .<sup>19</sup> This gives

$$I_\nu^{(d)} = \oint_\nu \int \frac{d^d \ell_1}{\pi^{d/2}} \cdots \int \frac{d^d \ell_{N_L}}{\pi^{d/2}} \exp \left[ - \sum_{j=1}^{N_k} \alpha_j D_j \right], \quad (\text{A.7})$$

where for brevity, we have defined the “Schwinger integral”

$$\oint_\nu := \int_0^\infty \frac{d\alpha_1 \alpha_1^{\nu_1-1}}{\Gamma(\nu_1)} \cdots \int_0^\infty \frac{d\alpha_{N_k} \alpha_{N_k}^{\nu_{N_k}-1}}{\Gamma(\nu_{N_k})}. \quad (\text{A.8})$$

Let us write [recall eq. (3.1)]

$$\sum_{j=1}^{N_k} \alpha_j D_j = \sum_{i,j=1}^{N_L} A_{ij} [\ell_i \cdot \ell_j] + 2 \sum_{i=1}^{N_L} B_i \cdot \ell_i + C, \quad (\text{A.9})$$

where  $B$  and  $C$  depend on the momenta  $p_j$ , and  $C$  also on the masses in the form  $-\sum_j \alpha_j m_j^2$ , whereas  $A$  is a constant matrix. By shifting  $\ell_{i=1}^{N_L} \rightarrow \ell_i - \sum_{j=1}^{N_L} A_{ij} B_j$  to complete the square in the exponential, one obtains a Gaussian integral that can be easily performed, leaving

$$I_\nu^{(d)} = \frac{1}{\pi^{N_L d/2}} \oint_\nu [\det(\pi A^{-1})]^{d/2} \exp \left[ \sum_{i,j=1}^{N_L} A_{ij}^{-1} B_i B_j - C \right] = \oint_\nu \frac{e^{-\mathcal{F}/\mathcal{U}+i\epsilon}}{\mathcal{U}^{d/2}}, \quad (\text{A.10})$$

where  $\mathcal{U} := \det(A)$  and  $\mathcal{F} := \mathcal{U}(\sum_{ij} A_{ij}^{-1} B_i B_j - C)$  are the *Symanzik polynomials*; they are polynomials in  $\{\alpha_j\}$  and are homogeneous of degree  $N_L$  and  $N_L + 1$ , respectively.<sup>20</sup>

Now, note that  $m_i^2$  only appears as the term  $\alpha_i m_i^2$  inside the exponent  $\mathcal{F}/\mathcal{U}$ , so the effect of  $\partial/\partial m_i^2$  on the right-hand side of eq. (A.10) is simply to bring down a factor of  $\alpha_i$  inside the integrand. Next, note that  $d$  only appears as the exponent in  $\mathcal{U}^{d/2}$ , and recall that  $\mathcal{U}$  is just a sum of products of  $\alpha_i$ ’s; explicitly, let us write it as  $\mathcal{U} =: U(\alpha_1, \alpha_2, \dots, \alpha_{N_k})$ . Then, maintaining that same functional form, it follows that

$$\mathcal{D} := U\left(\frac{\partial}{\partial m_1}, \frac{\partial}{\partial m_2}, \dots, \frac{\partial}{\partial m_{N_k}}\right) \quad (\text{A.11})$$

is a differential operator such that

$$\mathcal{D} I_\nu^{(d)} = \oint \frac{U(\alpha_1, \alpha_2, \dots, \alpha_{N_k}) e^{-\mathcal{F}/\mathcal{U}+i\epsilon}}{\mathcal{U}^{d/2}} = \oint \frac{e^{-\mathcal{F}/\mathcal{U}+i\epsilon}}{\mathcal{U}^{d/2-1}} = I_\nu^{(d-2)}. \quad (\text{A.12})$$

<sup>19</sup>Note that this assumes  $D > 0$ , which is only guaranteed in Euclidean space. However, since Wick rotation corresponds to a simple multiplicative factor for the integrals, the same identities hold also for the Minkowski-space integrals.

<sup>20</sup>We use the sign convention of `LiteRed` [49, 50] for the second Symanzik polynomial, which differs by a sign from the definition used in ref. [32].

On the other hand,  $\mathcal{D}I_{\vec{\nu}}^{(d)}$  is a linear combination of the  $d$ -dimensional master integrals. This produces a linear system that can be inverted to give the  $d$ -dimensional master integrals in terms of the less divergent  $(d-2)$ -dimensional ones. We present the relations for our case in sec. C.

A particularly elegant way of deriving  $\mathcal{D}$  is the well-known (see ref. [66]) graph-based determination of  $\mathcal{U}$ . Consider the graph  $G$  representing a given integral (as in fig. 1) and consider all ways of removing  $N_L$  edges from the graph in such a way that the remaining edges form a connected tree graph that joins all vertices, which is called a *spanning tree*. Then

$$\mathcal{U} = \sum_{\substack{\text{spanning} \\ \text{trees } T}} \prod_{j \in G \setminus T} \alpha_j, \quad (\text{A.13})$$

where  $G \setminus T$  is the set of  $N_L$  edges that were removed to form the spanning tree  $T$ . As above,  $\mathcal{D}$  is obtained by replacing  $\alpha_j \rightarrow \partial/\partial m_j^2$  in this formula. Sec. C details the application of this method to our master integrals.

### A.3 Schouten relations

An important thing to note is that the set of master integrals is only minimal and irreducible with respect to IBP relations. When working at fixed dimension or with fixed kinematics, additional relations may emerge that are not taken into account during master integral reduction. A simple example is how  $I_{\mathcal{Q}}$  (or  $E_0$ ) is trivially related to  $I_{\mathcal{O}}$  (or  $E_1$ ) by fixing  $t = 0$ , even though it is formally an independent master integral. However, the present amplitude involves less obvious relations, as can be inferred from renormalizability. Taking the sum of diagrams 91–101 in table 2 at face value, its divergent part contains the integrals  $E_n(2; t)$ ,<sup>21</sup> but since these are elliptic functions of  $t$ , no combination of rational functions and polylogarithms (which is what diagrams 00–90 provide) can cancel them. Thus, there must be some additional relation between the elliptic master integrals that makes this problematic divergence vanish.

Such subtle and novel relations indeed hold for  $E_5$  and  $E_6$ , and can be viewed as consequences of Schouten<sup>22</sup> identities; by analogy, we refer to these master integral relations as *Schouten relations*. Schouten identities hold only at fixed integer dimension, and while the relations can be extended to the  $\epsilon$  expansion around that dimension and translated to other dimensions through dimension shifting, they are not detected by the IBP relations, which operate in general  $d$ .<sup>23</sup> The role of Schouten identities in reducing the number of independent master integrals was first noticed by Remiddi & Tancredi [67] in the context of two-loop sunset integrals with three distinct masses, and is discussed further in ref. [38]. We have checked all relations numerically with `pySecDec` [51–54].

<sup>21</sup>The reason for this can be seen in sec. C, specifically eqs. (C.13) and (C.14), where the coefficients relating  $E_{5,6}(4-2\epsilon; t)$  to  $E_n(2-2\epsilon; t)$  diverge, introducing the finite integrals  $E_n(2; t)$  also into the divergent part. This is not the case for  $E_0$  through  $E_4$ .

<sup>22</sup>Pronounced [sxuqtən]. We make this point because difficult and oft-mangled names is a matter close to the heart of the author whose surname is pronounced [uqø:].

<sup>23</sup>We thank Roman Lee and Lorenzo Tancredi for discussions regarding this point.

In the remainder of this section, we will discuss Schouten relations from three angles, ranging from the more profoundly connected to its underlying cause, to the more practically applicable to the case at hand.

A Schouten identity is the statement that the Gram determinant of  $n$  vectors vanishes in  $d < n$  dimensions, since no more than  $d$  vectors may be linearly independent. In two dimensions, for three arbitrary vectors  $u, v$  and  $w$ , this takes the form

$$\mathbb{G}(u, v, w) := \begin{pmatrix} u^2 & u \cdot v & u \cdot w \\ v \cdot u & v^2 & v \cdot w \\ w \cdot u & w \cdot v & w^2 \end{pmatrix} \Rightarrow |\mathbb{G}(u, v, w)| = 0 \quad \text{at } d = 2. \quad (\text{A.14})$$

With  $u, v, w$  drawn from the loop and external momenta,  $|\mathbb{G}(u, v, w)|$  is a cubic polynomial in the  $D_j$  of eq. (3.1) which vanishes at  $d = 2$ . Inserting that as the numerator of a suitably chosen integral and reducing the result yields a ( $d = 2$ )-specific linear relation among the master integrals—a Schouten relation.

However, the above argument is only valid if the integral of interest is finite—the requirement that  $d = 2$  precludes dimensional regularization—and in most cases where a finite integral is obtained, the resulting linear combination is zero in any dimension, yielding no new information. However, a finite yet nontrivial result in our basis of propagators is obtained from  $I_{1,1,0,1,1,0,2,1,0}^{(d)}$  and  $|\mathbb{G}(\ell_1, \ell_2, \ell_3)|$ : the integral

$$G(d; t) := \int \frac{d^d \ell_1 d^d \ell_2 d^d \ell_3}{\pi^{3d/2}} \frac{|\mathbb{G}(\ell_1, \ell_2, \ell_3)|}{D_1 D_2 D_4 D_5 D_7^2 D_8} \quad (\text{A.15})$$

is finite at  $d = 2$  and reduces (using `LiteRed` [49, 50]) to

$$\begin{aligned} G(2; t) = & (t+8)(t-4)E_1(2; t) - (t^3 - 20t^2 - 128(t-1))E_2(2; t) - 2t(t-16)(t+4)E_3(2; t) \\ & - 12t(t+4)E_4(2; t) + 96(t-1)tE_5(2; t) - 48t^2(t-4)E_6(2; t) \\ & + \frac{24t}{(t-4)^2} [2 + J_{\infty}^{(1)}(t)] [t^2 + 8t - 16 + 4tJ_{\infty}^{(1)}(t)]. \end{aligned} \quad (\text{A.16})$$

On the other hand,  $G(2; t) = 0$  due to the presence of  $|\mathbb{G}(\ell_1, \ell_2, \ell_3)|$ . Using this removes all elliptic functions from the  $1/\epsilon^2$  pole of the 3-loop amplitude, which allows it to be canceled by the counterterms. However, the  $1/\epsilon$  pole contains  $E_i^{(1)}(2; t)$  [recall eq. (3.12)] and is therefore difficult to tame with similar integer-dimension methods.

A more systematic way of finding Schouten identities at any order in  $\epsilon$  comes from the differential equation for  $E_5$ . In two dimensions, the second-order differential operator factorizes into two first-order ones; the explicit expressions are given in eq. (B.9), but the schematic form is

$$\Delta_L \Delta_R E_5(2; t) = \mathcal{S}_5, \quad (\text{A.17})$$

where  $\Delta_{L,R}$  are linear differential operators and  $\mathcal{S}_5$  consists of integrals lower in the hierarchy of eq. (A.2). In fact, the same holds perturbatively in  $\epsilon$ :

$$\Delta_L \Delta_R E_5^{(r)}(2; t) = \mathcal{S}_5^{(r)}, \quad (\text{A.18})$$

where  $r$  denotes the order in  $\epsilon$  as given in eq. (3.12) and  $\mathcal{S}_5^{(r)}$  consists of integrals lower in the hierarchy and of  $E_5^{(r')}(2; t)$  and  $E_6^{(r')}(2; t)$  with  $r' < r$ .

Now, given  $\Sigma^{(r)}$  such that  $\Delta_L \Sigma^{(r)} = \mathcal{S}_5^{(r)}$ , we clearly get

$$\Delta_R E_5^{(r)}(2; t) = \Sigma^{(r)}, \quad (\text{A.19})$$

which is a linear differential equation; in fact, the  $r = 0$  version is the very same equation as that obtained through Griffiths-Dwork reduction [36, 37]. It can be contrasted with the plain derivative [explicitly, eq. (B.12)]

$$\frac{\partial}{\partial t} E_5^{(r)}(2; t) = \rho(t) E_6^{(r)}(2; t) + \tilde{\Sigma}^{(r)}, \quad (\text{A.20})$$

where  $\rho$  is a rational function and  $\tilde{\Sigma}^{(r)}$ , like  $\Sigma^{(r)}$ , is lower in the hierarchy or lower in the  $\epsilon$  expansion. Canceling  $\frac{\partial}{\partial t} E_5^{(r)}(2; t)$  between eqs. (A.19) and (A.20) gives a linear relation that for  $r = 0$  is equivalent to eq. (A.16). The lengthier  $r = 1$  version is, after eliminating  $E_6(2; t)$  with eq. (A.16),

$$\begin{aligned} 0 = & \frac{2}{9t} E_0(2) + \frac{(t-4)(5t+64)}{144t} E_1(2; t) + \frac{(t-4)(t+8)}{144t} E_1^{(1)}(2; t) \\ & + \frac{t^3 - 20t^2 + 128(2t-4)}{144t} E_2(2; t) - \frac{t^3 - 20t^2 + 128(t-1)}{144t} E_2^{(1)}(2; t) \\ & + \frac{(t+4)(t-16)}{36} \left( E_3(2; t) - \frac{1}{2} E_3^{(1)}(2; t) \right) + \frac{t-28}{12} E_4(2; t) - \frac{t+4}{12} E_4^{(1)}(2; t) \\ & - \frac{3t^2 - 36t + 16}{18} E_5(2; t) + \frac{2(t-1)}{3} E_5^{(1)}(2; t) - \frac{3}{t(t-4)} E_6^{(1)}(2; t) - \frac{2t}{(t-4)} \\ & - \frac{(t^2 + 16t - 16) J_{\infty}^{(2)}(t) (t^2 + 22t - 72) [J_{\infty}^{(1)}(t)]^2 + 4t J_{\infty}^{(1)}(t) [3t - 4 + 2J_{\infty}^{(2)}(t)]}{6(t-4)^2} \end{aligned} \quad (\text{A.21})$$

and eliminates the  $1/\epsilon$  pole in the same way that eq. (A.16) eliminated the  $1/\epsilon^2$  one. The procedure can in principle be carried on to all orders in  $\epsilon$ , but the challenge is the highly nontrivial step from  $\mathcal{S}^{(r)}$  to  $\Sigma^{(r)}$ . Nonetheless, this approach is interesting enough to warrant further study, since it can be applied to any master integral whose differential equation factorizes.

Ultimately, the most straightforward way of obtaining Schouten relations is to compare different ways of performing the  $\epsilon$  expansion. This obscures the origin of the relations and only works for the divergent part, but is sufficient for our purposes. Thus, we examine the expansions

$$\begin{aligned} E_5(4-2\epsilon; t) &= \frac{E_5^{(-3)}(4; t)}{\epsilon^3} + \frac{E_5^{(-2)}(4; t)}{\epsilon^2} + \frac{E_5^{(-1)}(4; t)}{\epsilon^1} + \mathcal{O}(\epsilon^0), \\ E_6(4-2\epsilon; t) &= \frac{E_6^{(-2)}(4; t)}{\epsilon^2} + \frac{E_6^{(-1)}(4; t)}{\epsilon^1} + \mathcal{O}(\epsilon^0), \end{aligned} \quad (\text{A.22})$$

where the values of  $E_{5,6}^{(-r)}(4; t)$  can be found by setting  $d = 4 - 2\epsilon$  in eqs. (C.13) and (C.14); this way, all but the  $1/\epsilon^3$  divergences contain elliptic master integrals. However, they can

also be found by plugging eq. (A.22) into the differential equations for  $E_5$  in eq. (B.9) and  $E_6$  in eq. (B.12), where much of the complexity diverts to the  $\mathcal{O}(\epsilon^0)$  terms. Inserting the  $\epsilon$  expansion for the lower-hierarchy integrals  $T_{21}$ ,  $T_{12}$ ,  $E_0$ ,  $E_1$ ,  $E_2$  and  $E_3$  near four dimensions given in secs. D.2 to D.5, we deduce that the coefficients of the poles of  $E_5$  and  $E_6$  can be written entirely in terms of  $J_{\circlearrowleft}^{(n)}(t)$ , as stated in eqs. (D.19) and (D.33). This is equivalent to eqs. (A.16) and (A.21).

The Schouten relations make it natural to express the amplitude in terms of  $\bar{E}_5(4; t)$  and  $\bar{E}_6(4; t)$ , since in two dimensions they eliminate  $E_6(2; t)$  and  $E_6^{(1)}(2; t)$  but leave more problematic functions like  $E_6^{(2)}(2; t)$ . Using the four-dimensional integrals becomes even more natural in the entirely four-dimensional approach of eq. (A.22). On the other hand, the integrals that are not the subject of Schouten relations— $E_0$  through  $E_4$ —are more naturally used in their finite two-dimensional form. This mixed two- and four-dimensional representation has the further benefit that  $E_4$  completely drops out of the expressions, as shown in sec. C.3.

## B Differential equations for the master integrals

In this section we present the differential equations satisfied by the master integrals (excluding the constants  $I_{\mathcal{Q}}$  and  $E_0$ ). The procedure for obtaining them is outlined in sec. A.1, and we will group them according to the hierarchy of eq. (A.2).

### B.1 Differential equations for tadpoles and bubbles

The bubble integral satisfies the first-order differential equation

$$\left[ t(t-4) \frac{\partial}{\partial t} - \frac{4+(d-4)t}{2} \right] I_{\circlearrowleft}(d; t) = (2-d) I_{\mathcal{Q}}(d), \quad (\text{B.1})$$

so it follows directly from eq. (3.8) that

$$\left[ t(t-4) \frac{\partial}{\partial t} - b \frac{4+(d-4)t}{2} \right] T_{ab}(d; t) = b(2-d) T_{a(b-1)}(d; t). \quad (\text{B.2})$$

At the level of  $J_{\circlearrowleft}^{(n)}(t)$ , eq. (B.1) translates to

$$\left[ t(t-4) \frac{\partial}{\partial t} - 2 \right] J_{\circlearrowleft}^{(n)}(t) = nt J_{\circlearrowleft}^{(n-1)}(t), \quad J_{\circlearrowleft}^{(0)}(t) = 1. \quad (\text{B.3})$$

### B.2 Differential equations for $E_1, E_2$ and $E_3$

The master  $E_1(d; t)$  satisfies the third-order differential equation [compare eq. (A.4)]

$$\left[ \pi_{13}(d; t) \frac{\partial^3}{\partial t^3} + \pi_{12}(d; t) \frac{\partial^2}{\partial t^2} + \pi_{11}(d; t) \frac{\partial}{\partial t} + \pi_{10}(d; t) \right] E_1(d; t) = -12(d-2)^3 T_{30}(d), \quad (\text{B.4})$$

with polynomial coefficients

$$\begin{aligned} \pi_{13}(d; t) &= 4(t-16)(t-4)t^2, \\ \pi_{12}(d; t) &= -12t[(d-4)t^2 - 10(d-5)t - 64], \\ \pi_{11}(d; t) &= (d-4)(11d-36)t^2 - 4(7d^2 - 88d + 216)t - 64(d-4)d, \\ \pi_{10}(d; t) &= -(d-3)(3d-8)[(d-4)t + 2d + 4]. \end{aligned} \quad (\text{B.5})$$

The masters  $E_2(d; t)$  and  $E_3(d; t)$  are obtained from the derivatives of  $E_1(d; t)$  using

$$E_2(d; t) = \left[ -\frac{t}{4} \frac{\partial}{\partial t} + \frac{3d-8}{8} \right] E_1(d; t), \quad (\text{B.6})$$

$$E_3(d; t) = \left[ \frac{t}{2} \frac{\partial^2}{\partial t^2} + \frac{4d+(4-d)t}{16} \frac{\partial}{\partial t} + \frac{(d-4)(3d-8)}{32} \right] E_1(d; t). \quad (\text{B.7})$$

Below, we often use this to eliminate  $E_2$  and  $E_3$  in favor of derivatives of  $E_1$ .

### B.3 Differential equation for $E_4$

The master  $E_4(d; t)$  satisfies the first-order differential equation

$$\left[ 2(4-t) \frac{\partial}{\partial t} + (4+(d-4)t) \right] E_4(d; t) = (d-2)E_0(d) + \left[ \frac{d-4}{2} - 3t \frac{\partial}{\partial t} \right] E_1(d; t). \quad (\text{B.8})$$

In fact, we do not use this equation here but include it for completeness.

### B.4 Differential equations for $E_5$ and $E_6$

The master  $E_5(d; t)$  satisfies the second-order differential equation

$$\begin{aligned} \left[ \pi_{52}(d; t) \frac{\partial^2}{\partial t^2} + \pi_{51}(d; t) \frac{\partial}{\partial t} + \pi_{50}(d; t) \right] E_5(d; t) &= \left[ \tilde{\pi}_{12}(d; t) \frac{\partial^2}{\partial t^2} + \tilde{\pi}_{11}(d; t) \frac{\partial}{\partial t} + \tilde{\pi}_{10}(d; t) \right] E_1(d; t) \\ &\quad - 24(d-3)(3d-8)E_4(d; t) + 6(3d-8)(d-2)E_0(d) \\ &\quad - 6(d-2)^2(t-2)T_{21}(d; t) + 12(d-3)(d-2)tT_{12}(d; t), \end{aligned} \quad (\text{B.9})$$

with polynomial coefficients

$$\begin{aligned} \pi_{52} &= 12(t-4)^2t^2, & \tilde{\pi}_{12} &= 2t(t+2)(t+8), \\ \pi_{51} &= -24(t-4)t[(d-5)t+11-2d], & \tilde{\pi}_{11} &= -(t+8)[(5d-16)t-2d], \\ \pi_{50} &= 3(t-4)[3(d-6)(d-4)t+8(2d-7)], & \tilde{\pi}_{10} &= (3d-8)[(d-3)t-2(2d-3)]. \end{aligned} \quad (\text{B.10})$$

It should be noted that the differential operator on the left-hand side of eq. (B.9) factorizes in two dimensions, with  $\epsilon$  corrections that are at most linear differential operators:

$$\begin{aligned} \left[ \pi_{52}(2-2\epsilon; t) \frac{\partial^2}{\partial t^2} + \pi_{51}(2-2\epsilon; t) \frac{\partial}{\partial t} + \pi_{50}(2-2\epsilon; t) \right] &= 12(t-4) \left[ t \frac{\partial}{\partial t} + 1 \right] \circ \left[ t(t-4) \frac{\partial}{\partial t} - 3(t-2) \right] \\ &\quad + \left[ 48(t-4)(2t-4) \frac{\partial}{\partial t} + 4(15t-8) \right] \epsilon + 12t\epsilon^2. \end{aligned} \quad (\text{B.11})$$

The implications of this are discussed in sec. A.3.

The master  $E_6(d; t)$  is obtained from the derivative of  $E_5(d; t)$  using

$$\begin{aligned} E_6(d; t) &= - \left[ \frac{\partial}{\partial t} + \frac{1}{t} \right] E_5(d; t) + \left[ \frac{t-16}{48(d-3)} \frac{\partial^2}{\partial t^2} - \frac{(5d-16)t+16d}{96(d-3)t} \frac{\partial}{\partial t} + \frac{3d-8}{96t} \right] E_1(d; t) \\ &\quad + \frac{3d-8}{8t} E_4(d; t) - \frac{(d-2)^2}{16(d-3)t} T_{21}(d; t). \end{aligned} \quad (\text{B.12})$$

## B.5 Initial conditions

When working with the above differential equations, it is useful to know the values of the master integrals at  $t = 0$ . Assuming the integrals to be sufficiently regular, this can be determined by setting  $q = 0$ , which following eq. (3.3) replaces  $\{D_4, D_5, D_6\} \rightarrow \{D_1, D_2, D_3\}$ , and then applying the master integral reduction. Since we have only two  $t$ -independent master integrals, the result must be of the form

$$E_i(d; 0) = \mu_i(d) E_0(d) + \tilde{\mu}_i(d) T_{30}(d), \quad (\text{B.13})$$

where<sup>24</sup>

$$\begin{aligned} \mu_1(d) &= 1, & \mu_2(d) = \mu_4(d) &= \frac{3d-8}{8}, & \tilde{\mu}_1(d) = \tilde{\mu}_2(d) = \tilde{\mu}_4(d) &= 0, \\ \mu_3(d) &= \frac{(d-7)(3d-10)(3d-8)}{128(d-4)}, & \tilde{\mu}_3(d) &= \frac{3(d-2)^3}{64(d-4)}, \\ \mu_5(d) &= \frac{(d-3)(3d-10)(3d-8)}{64(d-4)}, & \tilde{\mu}_5(d) &= -\frac{(d-2)^3}{32(d-4)}, \\ \mu_6(d) &= \frac{3(d-6)(d-3)(3d-10)(3d-8)}{1024(d-4)}, \\ \tilde{\mu}_6(d) &= \frac{(d-2)^3(5d-14)}{512(d-4)}. \end{aligned} \quad (\text{B.14})$$

Along with derivative relations such as eqs. (B.6), (B.7), and (B.12), this gives a complete set of initial conditions for the differential equations.

Expanding these relations near four dimensions and using the expansion of  $E_0(4-2\epsilon)$  given in eq. (D.10) and  $T_{30}(4-2\epsilon)$  given in eq. (D.9), we have

$$E_1(4-2\epsilon; 0) = \frac{2}{\epsilon^3} + \frac{23}{3\epsilon^2} + \frac{\pi^2 + 35}{2\epsilon} + \frac{275 + 23\pi^2 - 24\zeta(3)}{12} + \mathcal{O}(\epsilon), \quad (\text{B.15a})$$

$$E_2(4-2\epsilon; 0) = \frac{1}{\epsilon^3} + \frac{7}{3\epsilon^2} + \frac{12 + \pi^2}{4\epsilon} + \frac{7\pi^2}{12} - \zeta(3) - \frac{5}{3} + \mathcal{O}(\epsilon), \quad (\text{B.15b})$$

$$E_3(4-2\epsilon; 0) = -\frac{5}{6\epsilon^2} - \frac{5}{2\epsilon} - \frac{35}{6} - \frac{5\pi^2}{24} + \frac{7\zeta(3)}{2} + \mathcal{O}(\epsilon), \quad (\text{B.15c})$$

$$E_4(4-2\epsilon; 0) = E_2(4-2\epsilon; 0), \quad (\text{B.15d})$$

$$E_5(4-2\epsilon; 0) = \frac{1}{3\epsilon^3} + \frac{1}{3\epsilon^2} + \frac{4 + \pi^2}{12\epsilon} + \frac{1}{3} + \frac{\pi^2}{12} - \frac{8\zeta(3)}{3} + \mathcal{O}(\epsilon), \quad (\text{B.15e})$$

$$E_6(4-2\epsilon; 0) = -\frac{1}{4\epsilon^2} - \frac{1}{4\epsilon} - \frac{1}{4} - \frac{\pi^2}{16} + \frac{7\zeta(3)}{8} + \mathcal{O}(\epsilon). \quad (\text{B.15f})$$

We may also perform the expansion around  $t = 0$  of the finite master integrals to higher order by finding power-series solutions to the differential equations:

$$E_1(2; t) = -7\zeta(3) + \frac{6 - 7\zeta(3)}{16}t + \frac{54 - 49\zeta(3)}{1024}t^2 + \mathcal{O}(t^3), \quad (\text{B.16a})$$

---

<sup>24</sup>Despite the appearance of  $1/(d-4)$  multiplying the already cubically divergent integrals  $E_0$  and  $T_{30}$ , the quartic (and for  $E_3$  and  $E_6$ , also cubic) divergences cancel, as can be seen by combining eq. (B.13) with the expressions in sec. D.

$$E_2(2; t) = \frac{7\zeta(3)}{4} + \frac{7\zeta(3) - 6}{32}t + \frac{147\zeta(3) - 162}{4096}t^2 + \mathcal{O}(t^3), \quad (\text{B.16b})$$

$$E_3(2; t) = \frac{6 - 35\zeta(3)}{32} + \frac{102 - 105\zeta(3)}{512}t + \frac{458 - 399\zeta(3)}{8192}t^2 + \mathcal{O}(t^3), \quad (\text{B.16c})$$

$$\bar{E}_5(4; t) = \frac{1}{3} + \frac{\pi^2}{12} - \frac{8\zeta(3)}{3} + \left[ \frac{17}{96} - \frac{35}{64} + \frac{\pi^2}{24} \right]t + \mathcal{O}(t^2), \quad (\text{B.16d})$$

$$\bar{E}_6(4; t) = -\frac{1}{4} - \frac{\pi^2}{16} + \frac{7\zeta(3)}{8} + \left[ -\frac{\pi^2}{96} + \frac{1295\zeta(3)}{768} - \frac{23993}{31104} \right]t + \mathcal{O}(t^2). \quad (\text{B.16e})$$

## C Dimension-shifting relations

In this appendix we provide explicit expressions for the dimension-shifting relations derived using the methods described in sec. A.2. Since the tadpole and bubble integrals do not simplify significantly in two dimensions, we keep them four-dimensional and only apply the dimension shift to the  $E_i$ . We will express the relations using the notation

$$E_i(d; t) = \sum_{a,b} (d-2)^a \tau_i^{ab}(d; t) T_{ab}(d; t) + \sum_j \varepsilon_i^j(d; t) E_j(d-2; t), \quad (\text{C.1})$$

with the coefficients  $\tau_i^{ab}(d; t)$  and  $\varepsilon_i^j(d; t)$  given below, again grouped by the hierarchy eq. (A.2). Note that eq. (A.12) gives  $E_j(d-2; t)$  in terms of  $E_i(d; t)$ , so eq. (C.1) requires the inverse of that relation. We keep  $d$  general here; the  $\epsilon$  expansion around  $d = 4$  can be found in sec. D.

### C.1 Dimension shifting for the master $E_0$

This is a simple case that is good for familiarizing oneself with the method described in sec. A.2. The spanning trees (black, with removed lines grayed out) are

$$\text{Diagram 1} \quad \text{Diagram 2} \quad \text{Diagram 3} \quad \text{Diagram 4} \quad (\text{C.2})$$

Reading the line indices off fig. 1, eq. (A.13) gives

$$\mathcal{U} = \alpha_1 \alpha_2 \alpha_7 \alpha_8 \left( \frac{1}{\alpha_1} + \frac{1}{\alpha_2} + \frac{1}{\alpha_7} + \frac{1}{\alpha_8} \right), \quad (\text{C.3})$$

and the operator  $\mathcal{D}$  follows from  $\alpha_j \rightarrow \partial/\partial m_j^2$ . Running this through eq. (A.12) gives eq. (C.1) with coefficients

$$\kappa_0(d) \tau_0^{30}(d; t) = \frac{2(11d - 38)}{3}, \quad \kappa_0(d) \varepsilon_0^0(d; t) = \frac{128(d-4)}{3}, \quad (\text{C.4})$$

where we have pulled out a common denominator  $\kappa_0(d) := (d-3)(3d-10)(3d-8)$ . Here and below, we omit coefficients  $\tau_i^{ab}$  and  $\varepsilon_i^j$  that vanish identically. Note that since  $\varepsilon_0^0(d; t)$  vanishes at  $d = 4$ ,  $E_0(2)$  does not appear in  $E_0(4-2\epsilon)$  until the first order in  $\epsilon$ .

## C.2 Dimension shifting for the masters $E_1$ , $E_2$ and $E_3$

Here,  $\mathcal{U}$  and  $\mathcal{D}$  are the same as for  $E_0$ , except that index 2 is replaced by 5; compare fig. 1. The resulting coefficients in eq. (C.1) for  $E_1$  are

$$\kappa_1(d)\tau_1^{30}(d; t) = \frac{(d-4)^2}{48}t^2 + \frac{11d^2 - 85d + 164}{6}t + \frac{2(38d^2 - 268d + 473)}{3}, \quad (\text{C.5a})$$

$$\begin{aligned} \kappa_1(d)\varepsilon_1^1(d; t) = & \frac{5d^2 - 47d + 110}{24}t^3 + \frac{2(15d^2 - 128d + 275)}{3}t^2 - \frac{2(276d^2 - 2342d + 5027)}{3}t \\ & - \frac{32(20d^2 - 178d + 385)}{3} + \frac{512(3d^2 - 26d + 56)}{3}\frac{1}{t}, \end{aligned} \quad (\text{C.5b})$$

$$\begin{aligned} \kappa_1(d)\varepsilon_1^2(d; t) = & \frac{d-6}{24}t^4 + \frac{d-10}{6}t^3 - \frac{2(97d - 487)}{3}t^2 \\ & + \frac{16(73d - 354)}{3}t + \frac{128(29d - 119)}{3} - \frac{4096(d-4)}{3}\frac{1}{t-4}, \end{aligned} \quad (\text{C.5c})$$

$$\kappa_1(d)\varepsilon_1^3(d; t) = -\frac{1}{6}t^4 - \frac{10}{3}t^3 + 112t^2 - \frac{640}{3}t - \frac{2048}{3}, \quad (\text{C.5d})$$

with  $\kappa_1(d) := (d-3)(2d-7)(2d-5)(3d-10)(3d-8)$ .

Those for  $E_2$  are

$$\kappa_2(d)\tau_2^{30}(d; t) = \frac{9d^2 - 70d + 136}{48}t + \frac{54d^2 - 383d + 680}{12}, \quad (\text{C.6a})$$

$$\begin{aligned} \kappa_2(d)\varepsilon_2^1(d; t) = & \frac{(33d^2 - 295d + 662)}{24}t^2 + \frac{(-108d^2 + 921d - 1996)}{6} \\ & - 8(9d^2 - 80d + 175) + \frac{128(3d^2 - 26d + 56)}{3}\frac{1}{t}, \end{aligned} \quad (\text{C.6b})$$

$$\begin{aligned} \kappa_2(d)\varepsilon_2^2(d; t) = & \frac{5(d-6)}{24}t^3 + \frac{254 - 49d}{6}t^2 + \frac{2(33d - 179)}{3}t \\ & + \frac{32(31d - 131)}{3} - \frac{1024(d-4)}{3}\frac{1}{t}, \end{aligned} \quad (\text{C.6c})$$

$$\kappa_2(d)\varepsilon_2^3(d; t) = t^3 + 14t^2 - \frac{512}{3}, \quad (\text{C.6d})$$

with  $\kappa_2(d) := (d-3)(2d-7)(3d-10)(3d-8)$ , and those for  $E_3$  are

$$\kappa_3(d)\tau_3^{30}(d; t) = \frac{(d-4)^2}{32}t + \frac{69d^3 - 753d^2 + 2732d - 3296}{48(2d-7)}, \quad (\text{C.7a})$$

$$\begin{aligned} \kappa_3(d)\varepsilon_3^1(d; t) = & \frac{6d^2 - 55d + 126}{24}t^2 + \frac{-111d^3 + 1454d^2 - 6270d + 8896}{24(2d-7)}t \\ & + \frac{-264d^3 + 3077d^2 - 11907d + 15288}{6(2d-7)} \\ & + \frac{8(21d^3 - 254d^2 + 1016d - 1344)}{3(2d-7)}\frac{1}{t}, \end{aligned} \quad (\text{C.7b})$$

$$\begin{aligned} \kappa_3(d)\varepsilon_3^2(d; t) = & \frac{d-6}{24}t^3 + \frac{-73d^2 + 646d - 1368}{24(2d-7)}t^2 + \frac{21d^2 - 264d + 676}{6(2d-7)}t \\ & + \frac{10(47d^2 - 355d + 664)}{3(2d-7)} - \frac{64(7d^2 - 52d + 96)}{3(2d-7)}\frac{1}{t}, \end{aligned} \quad (\text{C.7c})$$

$$\kappa_3(d)\varepsilon_3^3(d; t) = -\frac{1}{6}t^3 + \frac{33d-116}{6(2d-7)}t^2 + \frac{2(3d-8)}{3(2d-7)}t - \frac{32(7d-24)}{3(2d-7)}, \quad (\text{C.7d})$$

with  $\kappa_3(d) := (d-3)(3d-10)(3d-8)$ .

### C.3 Dimension shifting for the master $E_4$

Here, the spanning trees are



$$\text{ (C.8)}$$

giving

$$\mathcal{U} = \alpha_2\alpha_7\alpha_8 \left[ 1 + (\alpha_1 + \alpha_4) \left( \frac{1}{\alpha_2} + \frac{1}{\alpha_7} + \frac{1}{\alpha_8} \right) \right]. \quad (\text{C.9})$$

The coefficients are

$$\kappa_4(d)\tau_4^{30}(d; t) = \frac{(d-4)^2}{48}t - \frac{16d^2 - 115d + 207}{6}, \quad (\text{C.10a})$$

$$\kappa_4(d)\tau_4^{21}(d; t) = \frac{(d-3)(2d-7)(11d-38)}{2}, \quad (\text{C.10b})$$

$$\kappa_4(d)\varepsilon_4^0(d; t) = \frac{32(d-4)(2d-7)}{3}, \quad (\text{C.10c})$$

$$\begin{aligned} \kappa_4(d)\varepsilon_4^1(d; t) = & \frac{5d^2 - 47d + 110}{24}t^2 + \frac{-24d^2 + 263d - 678}{6}t \\ & + \frac{8(37d^2 - 320d + 693)}{3} - \frac{128(3d^2 - 26d + 56)}{3}\frac{1}{t}, \end{aligned} \quad (\text{C.10d})$$

$$\begin{aligned} \kappa_4(d)\varepsilon_4^2(d; t) = & \frac{d-6}{24}t^3 + \frac{74-13d}{6}t^2 + \frac{2(61d-315)}{3}t \\ & - 32(9d-41) + \frac{1024(d-4)}{3}\frac{1}{t}, \end{aligned} \quad (\text{C.10e})$$

$$\kappa_4(d)\varepsilon_4^3(d; t) = -\frac{1}{6}t^3 + 6t^2 - 64t + \frac{512}{3}, \quad (\text{C.10f})$$

$$\kappa'_4(d)\varepsilon_4^4(d; t) = -\frac{32(d-4)}{3}t + \frac{128(d-4)}{3}, \quad (\text{C.10g})$$

with  $\kappa_4(d) := (d-3)^2(2d-7)(3d-10)(3d-8)$  and  $\kappa'_4(d) := (d-3)^2(9d^2 - 54d + 80)$ .

An interesting thing to note here is that  $\varepsilon_4^4(4; t) = 0$ , so  $E_4(2; t)$  is not needed in order to evaluate  $\bar{E}_4(4; t)$ . This does not necessarily mean that  $E_4$  is eliminated by the dimension shift, though, since it still appears in  $E_5$  and  $E_6$  (see below) as well as in  $E_i^{(r)}(4; t)$  for  $r > 0$ . However, this is why it does not appear in eq. (4.5).

### C.4 Dimension shifting for the masters $E_5$ and $E_6$

Here, the spanning trees are



$$\text{ (C.11)}$$

plus horizontal and vertical reflections thereof. Thus,

$$\mathcal{U} = \alpha_7\alpha_8 [\alpha_1 + \alpha_2 + \alpha_4 + \alpha_5] + (\alpha_7 + \alpha_8) [\alpha_1\alpha_5 + \alpha_2\alpha_4 + \alpha_1\alpha_4 + \alpha_2\alpha_5]. \quad (\text{C.12})$$

The coefficients are

$$\begin{aligned}\kappa_5(d; t)\tau_5^{30}(d; t) = & -\frac{(d-4)^3}{96(d-5)(d-3)^2}t^4 + \frac{(d-4)^2}{24(d-3)^2}t^3 \\ & + \frac{9d^5 - 191d^4 + 1613d^3 - 6755d^2 + 14002d - 11480}{12(d-5)(d-3)^2(2d-7)(3d-10)}t^2 \\ & + \frac{-72d^4 + 1075d^3 - 5981d^2 + 14700d - 13468}{3(d-3)^2(6d^2 - 41d + 70)}t \\ & + \frac{4(d-4)^2(39d^2 - 261d + 434)}{3(d-3)^2(6d^2 - 41d + 70)},\end{aligned}\quad (\text{C.13a})$$

$$\begin{aligned}\kappa_5(d; t)\tau_5^{21}(d; t) = & \frac{(d-4)^3}{48(d-5)(d-3)}t^4 - \frac{(d-4)^2}{12(d-3)}t^3 + \frac{-7d^3 + 100d^2 - 475d + 748}{6(d^2 - 8d + 15)}t^2 \\ & + \frac{4(15d^2 - 125d + 258)}{3(d-3)}t - \frac{8(5d^2 - 41d + 84)}{d-3},\end{aligned}\quad (\text{C.13b})$$

$$\begin{aligned}\kappa_5(d; t)\tau_5^{12}(d; t) = & \frac{8(d^2 - 9d + 20)}{3}t^2 - \frac{4(23d^2 - 195d + 410)}{3}t \\ & + \frac{16(11d^2 - 93d + 196)}{3},\end{aligned}\quad (\text{C.13c})$$

$$\kappa'_5(d)\varepsilon_5^0(d; t) = \frac{2(d-4)^3}{3}t + \frac{8(d-4)^2}{9} - \frac{16(d-4)(27d^2 - 217d + 434)}{9(3d-10)}\frac{1}{t}, \quad (\text{C.13d})$$

$$\begin{aligned}\kappa'_5(d)\varepsilon_5^1(d; t) = & \frac{8(d^2 - 9d + 20)}{3}t^2 - \frac{4(23d^2 - 195d + 410)}{3}t \\ & + \frac{16(11d^2 - 93d + 196)}{3},\end{aligned}\quad (\text{C.13e})$$

$$\begin{aligned}\kappa'_5(d)\varepsilon_5^2(d; t) = & -\frac{(d-6)(d-4)^2}{144(d-5)}t^4 + \frac{10d^3 - 133d^2 + 586d - 856}{36(d-5)}t^3 \\ & + \frac{-9d^5 + 327d^4 - 3821d^3 + 20111d^2 - 49728d + 47180}{18(d-5)(2d-7)(3d-10)}t^2 \\ & + \frac{2(177d^4 - 2798d^3 + 16759d^2 - 45116d + 46060)}{9(6d^2 - 41d + 70)}t \\ & + \frac{8(111d^4 - 1339d^3 + 5186d^2 - 5760d - 2688)}{9(6d^2 - 41d + 70)} \\ & - \frac{128(54d^4 - 810d^3 + 4537d^2 - 11245d + 10402)}{9(6d^2 - 41d + 70)}\frac{1}{t},\end{aligned}\quad (\text{C.13f})$$

$$\begin{aligned}\kappa'_5(d)\varepsilon_5^3(d; t) = & \frac{(d-4)^2}{36(d-5)}t^4 + \frac{-4d^2 + 33d - 68}{9(d-5)}t^3 \\ & + \frac{2(9d^4 - 201d^3 + 1499d^2 - 4669d + 5250)}{9(d-5)(2d-7)(3d-10)}t^2 \\ & - \frac{8(33d^3 - 422d^2 + 1809d - 2590)}{9(6d^2 - 41d + 70)}t - \frac{128(3d^3 - 10d^2 - 53d + 182)}{9(6d^2 - 41d + 70)},\end{aligned}\quad (\text{C.13g})$$

$$\frac{\kappa'_5(d)}{3d-14}\varepsilon_5^4(d; t) = \frac{(d-4)^2}{12}t^3 - \frac{(2d^2 - 17d + 36)}{3}t^2 + \frac{2(2d^2 - 17d + 35)}{3}t$$

$$+ \frac{8(4d^2 - 31d + 59)}{3}, \quad (\text{C.13h})$$

$$\begin{aligned} \kappa'_5(d)\varepsilon_5^5(d; t) = & -\frac{(d-6)(d-4)^2}{3}t^3 + 2(d^3 - 15d^2 + 74d - 120)t^2 \\ & - \frac{8(9d^3 - 121d^2 + 536d - 780)}{3}t + \frac{32(4d^3 - 52d^2 + 223d - 315)}{3}, \end{aligned} \quad (\text{C.13i})$$

$$\begin{aligned} \kappa'_5(d)\varepsilon_5^6(d; t) = & -\frac{2(d-4)^2}{3}t^4 + \frac{8(2d^2 - 17d + 36)}{3}t^3 - \frac{16(4d^2 - 35d + 75)}{3}t^2 \\ & + \frac{64(2d^2 - 17d + 35)}{3}t, \end{aligned} \quad (\text{C.13j})$$

with  $\kappa_5(d; t) := (d-4)(3d-14)(3d-10)(t-4)^2$  and  $\kappa'_5(d) := (d-4)^2(d-3)^2(3d-14)(3d-10)$ . For  $E_6$ , they are

$$\begin{aligned} \kappa_6(d; t)\tau_6^{30}(d; t) = & \frac{(d-4)^2(3d-10)}{192(d-3)}t^3 + \frac{-3d^3 + 37d^2 - 150d + 200}{96(d-3)}t^2 \\ & + \frac{-21d^3 + 274d^2 - 1185d + 1690}{24(d-3)}t + \frac{24d^3 - 311d^2 + 1329d - 1870}{6(d-3)}, \end{aligned} \quad (\text{C.14a})$$

$$\begin{aligned} \kappa_6(d; t)\tau_6^{21}(d; t) = & -\frac{(d-4)^2(3d-10)}{96}t^3 + \frac{(3d^3 - 37d^2 + 150d - 200)}{48}t^2 \\ & + \frac{1}{12}(45d^3 - 594d^2 + 2585d - 3690)t - 18d^3 + 233d^2 - 993d + 1390, \end{aligned} \quad (\text{C.14b})$$

$$\kappa_6(d; t)\tau_6^{12}(d; t) = -\frac{4(d-5)^2(d-3)(3d-10)}{3}t + \frac{4(d-5)(d-3)(3d-10)(5d-23)}{3}, \quad (\text{C.14c})$$

$$\kappa'_6(d)\varepsilon_6^0(d; t) = -\frac{(d-4)^2}{3} + \frac{2(d-4)(9d^2 - 87d + 206)}{9(3d-10)}\frac{1}{t}, \quad (\text{C.14d})$$

$$\begin{aligned} \kappa'_6(d)\varepsilon_6^1(d; t) = & \frac{6d^3 - 79d^2 + 346d - 504}{288(d-5)}t^2 + \frac{6d^3 - 73d^2 + 291d - 378}{144(d-5)}t \\ & + \frac{63d^3 - 714d^2 + 2670d - 3292}{36(3d-10)} + \frac{4(36d^3 - 465d^2 + 1997d - 2850)}{9(3d-10)}\frac{1}{t}, \end{aligned} \quad (\text{C.14e})$$

$$\begin{aligned} \kappa'_6(d)\varepsilon_6^2(d; t) = & \frac{d^2 - 10d + 24}{288(d-5)}t^3 + \frac{-19d^2 + 175d - 398}{144(d-5)}t^2 + \frac{-11d^2 + 93d - 186}{36(d-5)}t \\ & - \frac{2(3d^2 + 14d - 88)}{9(3d-10)} - \frac{16(27d^2 - 225d + 466)}{9(3d-10)}\frac{1}{t}, \end{aligned} \quad (\text{C.14f})$$

$$\kappa'_6(d)\varepsilon_6^3(d; t) = \frac{4-d}{72(d-5)}t^3 + \frac{7d-29}{36(d-5)}t^2 + \frac{5d-17}{9(d-5)}t - \frac{16}{9}, \quad (\text{C.14g})$$

$$\kappa'_6(d)\varepsilon_6^4(d; t) = -\frac{(d-4)(3d-14)}{24}t^2 + \frac{(3d-14)(3d-13)}{12}t - \frac{(3d-14)(d^2 - 7d + 14)}{3(3d-10)}, \quad (\text{C.14h})$$

$$\kappa'_6(d)\varepsilon_6^5(d;t) = \frac{(d^2 - 10d + 24)}{6}t^2 - \frac{2(d^2 - 11d + 30)}{3}t + \frac{4(2d^2 - 19d + 45)}{3}, \quad (\text{C.14i})$$

$$\kappa'_6(d)\varepsilon_6^6(d;t) = \frac{d-4}{3}t^3 - \frac{2(3d-13)}{3}t^2 + \frac{8(d-5)}{3}t, \quad (\text{C.14j})$$

with  $\kappa_6(d;t) := (d-5)(d-4)(3d-14)(3d-10)(t-4)^2$  and  $\kappa'_6(d) := (d-4)(d-3)^2(3d-14)$ .

Note that, unlike  $\varepsilon_0^j$  through  $\varepsilon_4^j$ , the coefficients  $\varepsilon_5^j(d;t)$  and  $\varepsilon_6^j(d;t)$  diverge at  $d = 4$ . This is why  $E_i$  appear in the divergent parts of  $E_5(4-2\epsilon; t)$  and  $E_6(4-2\epsilon; t)$ , the implications of which are discussed in sec. A.3. Note also that  $\tau_5^{ab}$  and  $\tau_6^{ab}$  diverge at the 2-pion threshold,  $t = 4$ . This potentially problematic behavior is also remedied by the Schouten relations.

## D Expressions for the master integrals in $d = 4 - 2\epsilon$ dimensions

In this section we give the expressions for the master integrals in  $d = 4 - 2\epsilon$  dimensions which are needed for the evaluation of the amplitude.

### D.1 The one-loop bubble in $d = 4 - 2\epsilon$

Restating eqs. (3.6) and (3.7), we express the bubble as

$$I_{\infty}(4-2\epsilon; t) = \frac{i \exp \left[ \sum_{k=2}^{\infty} (-\epsilon)^k \frac{\zeta(k)}{k} \right]}{\epsilon} \left[ 1 + \sum_{n=1}^{\infty} (-\epsilon)^n \frac{J_{\infty}^{(n)}(t)}{n!} \right], \quad (\text{D.1})$$

where  $\zeta(k)$  is the Riemann zeta function and

$$J_{\infty}^{(n)}(t) := \int_0^1 dx \log^n [1 - x(1-x)t]. \quad (\text{D.2})$$

Setting  $t = 4/(1 - \beta^2)$ , in the region where  $t < 0$  we have  $\beta^2 > 1$  and choose the branch  $\beta > 1$ . In terms of this, the differential equation eq. (B.3) is

$$(1 - \beta^2) \left( \beta \frac{\partial}{\partial \beta} - 1 \right) J_{\infty}^{(n)}(\beta) = 2n J_{\infty}^{(n-1)}(\beta), \quad J_{\infty}^{(0)}(\beta) = 0. \quad (\text{D.3})$$

This can be solved in terms of the polylogarithms [68, (5.4.1)]

$$\text{Li}_1(z) := -\log(1-z), \quad \text{Li}_{r+1}(z) := \int_0^z \frac{dt}{t} \text{Li}_r(t), \quad (\text{D.4})$$

and the  $\epsilon$  orders needed for the evaluations in this work read

$$J_{\infty}^{(1)}(\beta) = \beta \left[ \log(\beta_+) - \log(\beta_-) \right] - 2, \quad (\text{D.5a})$$

$$J_{\infty}^{(2)}(\beta) = 8 - 2\beta \left[ f_2(\beta_+) - f_2(\beta_-) \right],$$

$$f_2(z) := \text{Li}_2(z) + \frac{1}{2} \log(z)^2 + 2 \log(z), \quad (\text{D.5b})$$

$$J_{\infty}^{(3)}(\beta) = -48 + 12\beta \left[ f_3(\beta_+) - f_3(\beta_-) \right] + 3\beta \log(\beta_+) \log(\beta_-) \left[ \log(\beta_+) - \log(\beta_-) \right],$$

$$f_3(z) := \text{Li}_3(z) + \frac{1}{12} \log(z)^3 - \frac{\pi^2}{12} \log(z) + f_2(z), \quad (\text{D.5c})$$

where we have introduced the notation

$$\beta_+ := \frac{\beta+1}{2\beta} \in [1, \frac{1}{2}]; \quad \beta_- := \frac{\beta-1}{2\beta} \in [0, \frac{1}{2}], \quad \beta \geq 1. \quad (\text{D.6})$$

Although derived for  $t < 0$ , the expressions given here hold in the entire complex plane except for a branch cut along  $\beta \in [-1, 1]$ , i.e.,  $t \in [4, \infty)$ , as is expected from the cut of the amplitude.

Around  $\beta = \infty$  (i.e.,  $t = 0$ ),  $J_{\circlearrowleft}^{(n)}(\beta)$  has the series expansions

$$J_{\circlearrowleft}^{(1)}(\beta) = \sum_{n=1}^{\infty} \frac{2}{(2n+1)\beta^{2n}} = \sum_{n=1}^{\infty} \frac{-t^n n!(n-1)!}{(2n+1)!}, \quad (\text{D.7a})$$

$$J_{\circlearrowleft}^{(2)}(\beta) = \frac{8}{15\beta^4} + \frac{64}{105\beta^6} + \frac{568}{945\beta^8} + \mathcal{O}(\beta^{-10}) = \frac{t^2}{30} + \frac{t^3}{140} + \frac{11t^4}{7560} + \mathcal{O}(t^5), \quad (\text{D.7b})$$

$$J_{\circlearrowleft}^{(3)}(\beta) = \frac{16}{35\beta^6} + \frac{16}{21\beta^8} + \mathcal{O}(\beta^{-10}) = -\frac{t^3}{140} - \frac{t^4}{420} + \mathcal{O}(t^5). \quad (\text{D.7c})$$

## D.2 The tadpole-bubble products in $d = 4 - 2\epsilon$ dimensions

In this section we state the master integrals defined in eqs. (3.9) and (3.10), which following eq. (3.8) can be expressed in terms of the one-loop tadpole [eq. (3.5)] and bubble [eqs. (3.6) and (3.7)] integrals. We state their  $\epsilon$  expansion to the order needed in this work, which is driven by the presence of  $1/\epsilon$  counterterms in the two-loop diagrams, and the presence of  $T_{30}$  in the divergences of the  $E_i$ . The two-loop masters are

$$T_{20}(4-2\epsilon) = \frac{1}{\epsilon^2} + \frac{2}{\epsilon} + \left[ 3 + \frac{\pi^2}{6} \right] + \left[ 4 + \frac{\pi^2}{3} - \frac{2}{3}\zeta(3) \right] \epsilon + \mathcal{O}(\epsilon^2), \quad (\text{D.8a})$$

$$\begin{aligned} T_{11}(4-2\epsilon; t) = & \frac{1}{\epsilon^2} + \frac{1 - J_{\circlearrowleft}^{(1)}(t)}{\epsilon} + \left[ 1 + \frac{\pi^2}{6} - J_{\circlearrowleft}^{(1)}(t) + \frac{1}{2}J_{\circlearrowleft}^{(2)}(t) \right] \\ & + \left[ 1 + \frac{\pi^2}{6} - \frac{2}{3}\zeta(3) - \left( 1 + \frac{\pi^2}{6} \right) J_{\circlearrowleft}^{(1)}(t) + \frac{1}{2}J_{\circlearrowleft}^{(2)}(t) - \frac{1}{6}J_{\circlearrowleft}^{(3)}(t) \right] \epsilon \\ & + \mathcal{O}(\epsilon^2), \end{aligned} \quad (\text{D.8b})$$

$$\begin{aligned} T_{02}(4-2\epsilon; t) = & \frac{1}{\epsilon^2} - \frac{2J_{\circlearrowleft}^{(1)}(t)}{\epsilon} + \left[ \frac{\pi^2}{6} + [J_{\circlearrowleft}^{(1)}(t)]^2 + J_{\circlearrowleft}^{(2)}(t) \right] \\ & - \left[ \frac{2}{3}\zeta(3) + \left[ \frac{\pi^2}{3} - J_{\circlearrowleft}^{(2)}(t) \right] J_{\circlearrowleft}^{(2)}(t) + \frac{1}{3}J_{\circlearrowleft}^{(3)}(t) \right] \epsilon + \mathcal{O}(\epsilon^2), \end{aligned} \quad (\text{D.8c})$$

and the three-loop ones are

$$\begin{aligned} T_{30}(4-2\epsilon) = & \frac{1}{\epsilon^3} + \frac{3}{\epsilon^2} + \frac{24+\pi^2}{4\epsilon} + \left[ 10 + \frac{3\pi^2}{4} - \zeta(3) \right] + \left[ 15 + \frac{3\pi^2}{2} + \frac{19\pi^4}{480} - 3\zeta(3) \right] \epsilon \\ & + \left[ 21 + \frac{5\pi^2}{2} + \frac{19\pi^4}{160} - \left( 6 + \frac{\pi^2}{4} \right) \zeta(3) - \frac{3}{5}\zeta(5) \right] \epsilon^2 + \mathcal{O}(\epsilon^3), \end{aligned} \quad (\text{D.9a})$$

$$\begin{aligned} T_{21}(4-2\epsilon; t) = & \frac{1}{\epsilon^3} + \frac{2 - J_{\circlearrowleft}^{(1)}(t)}{\epsilon^2} + \frac{12 + \pi^2 - 8J_{\circlearrowleft}^{(1)}(t) + 2J_{\circlearrowleft}^{(2)}(t)}{4\epsilon} \\ & + \left[ 4 + \frac{\pi^2}{2} - \zeta(3) - \left( 3 + \frac{\pi^2}{4} \right) J_{\circlearrowleft}^{(1)}(t) + J_{\circlearrowleft}^{(2)}(t) - \frac{1}{6}J_{\circlearrowleft}^{(3)}(t) \right] + \mathcal{O}(\epsilon), \end{aligned} \quad (\text{D.9b})$$

$$T_{12}(4-2\epsilon; t) = \frac{1}{\epsilon^3} + \frac{1 - 2J_{\circlearrowleft}^{(1)}(t)}{\epsilon^2} + \frac{4 + \pi^2 - 8J_{\circlearrowleft}^{(1)}(t) + 4[J_{\circlearrowleft}^{(1)}(t)]^2 + 4J_{\circlearrowleft}^{(2)}(t)}{4\epsilon}$$

$$\begin{aligned}
& + \left[ 1 + \frac{\pi^2}{4} - \zeta(3) - \left( 2 + \frac{\pi^2}{2} \right) J_{\infty}^{(1)}(t) + [J_{\infty}^{(1)}(t)]^2 + [1 - J_{\infty}^{(1)}(t)] J_{\infty}^{(2)}(t) \right. \\
& \quad \left. - \frac{1}{3} J_{\infty}^{(3)}(t) \right] + \mathcal{O}(\epsilon), \tag{D.9c}
\end{aligned}$$

$$\begin{aligned}
T_{03}(4 - 2\epsilon; t) = & \frac{1}{\epsilon^3} - \frac{3J_{\infty}^{(1)}(t)}{\epsilon^2} + \frac{\pi^2 + 12[J_{\infty}^{(1)}(t)]^2 + 6J_{\infty}^{(2)}(t)}{4\epsilon} \\
& - \left[ \zeta(3) + [J_{\infty}^{(1)}(t)]^3 + 3\left[\frac{\pi^2}{4} - J_{\infty}^{(2)}(t)\right] J_{\infty}^{(1)}(t) + \frac{1}{2} J_{\infty}^{(3)}(t) \right] + \mathcal{O}(\epsilon). \tag{D.9d}
\end{aligned}$$

### D.3 The master integral $E_0$ in $d = 4 - 2\epsilon$

The expansion of  $E_0(4 - 2\epsilon)$  is easily worked out from the parametric representation of the integral and using `HyperInt` [69], or by evaluating the expression in ref. [70, eq. (5.48)] using that  $\omega_d = 2\pi^{\frac{d}{2}}/\Gamma(\frac{d}{2})$ , or by setting  $t = 0$  in the expressions for  $E_1(4 - 2\epsilon; t)$  below, or directly from the dimensional shift in eq. (C.4), requiring only knowledge of  $T_{30}(4 - 2\epsilon)$ . In any case,

$$\begin{aligned}
E_0(4 - 2\epsilon) = & \frac{2}{\epsilon^3} + \frac{23}{3\epsilon^2} + \frac{\pi^2 + 35}{2\epsilon} + \frac{275 + 23\pi^2 - 24\zeta(3)}{12} \\
& + \left( \frac{89\zeta(3)}{3} + \frac{19\pi^4}{240} + \frac{35\pi^2}{8} - \frac{189}{8} \right) \epsilon + \mathcal{O}(\epsilon^2). \tag{D.10}
\end{aligned}$$

### D.4 The master integrals $E_1$ , $E_2$ and $E_3$ in $d = 4 - 2\epsilon$

We expand these master integrals by directly applying the dimension shifting relations in eqs. (C.5), (C.6), and (C.7), utilizing the fact that  $E_i(2; t)$  are all finite. For  $E_1$ , we get

$$E_1(4 - 2\epsilon; t) = \frac{2}{\epsilon^3} + \frac{23 - t}{3\epsilon^2} + \frac{t^2 - 54t + 18\pi^2 + 630}{36\epsilon} + \bar{E}_1(4; t) + \mathcal{O}(\epsilon), \tag{D.11}$$

where the finite piece at order  $\epsilon^0$  is

$$\begin{aligned}
\bar{E}_1(4; t) = & \frac{t^3 + 24t^2 - 600t + 896}{288} E_1(2; t) - \frac{t^4 + 12t^3 - 792t^2 + 3968t + 1536}{288} E_2(2; t) \\
& - \frac{(t - 16)(t - 4)(t^2 + 40t + 64)}{144} E_3(2; t) + \frac{71t^2 + 18t + 6102}{216} + \frac{(23 - t)\pi^2}{12} - 2\zeta(3). \tag{D.12}
\end{aligned}$$

Likewise for  $E_2$ ,

$$E_2(4 - 2\epsilon; t) = \frac{1}{\epsilon^3} + \frac{28 - t}{12\epsilon^2} + \frac{24 - t + 2\pi^2}{8\epsilon} + \bar{E}_2(4; t) + \mathcal{O}(\epsilon), \tag{D.13}$$

with the finite piece

$$\begin{aligned}
\bar{E}_2(4; t) = & \frac{5t^2 - 80t + 96}{96} E_1(2; t) - \frac{5t^3 - 116t^2 + 376t + 896}{96} E_2(2; t) \\
& - \frac{(t - 16)(t - 4)(5t + 16)}{48} E_3(2; t) + \frac{(95t + 112) + (28 - t)\pi^2}{48} - \zeta(3), \tag{D.14}
\end{aligned}$$

and lastly for  $E_3$ ,

$$E_3(4 - 2\epsilon; t) = -\frac{5}{6\epsilon^2} + \frac{t - 20}{8\epsilon} + \bar{E}_3(4; t) + \mathcal{O}(\epsilon), \tag{D.15}$$

with the finite piece

$$\begin{aligned}\bar{E}_3(4; t) = & \frac{t^2 - 12t - 8}{96} E_1(2; t) - \frac{t^3 - 24t^2 + 88t + 160}{96} E_2(2; t) \\ & - \frac{(t - 16)(t - 4)(t + 4)}{48} E_3(2; t) + \frac{39t - 232 - 10\pi^2}{48}.\end{aligned}\quad (\text{D.16})$$

The expressions for the two-dimensional elliptic master integrals are given in sec. E.

### D.5 The master integral $E_4$ in $d = 4 - 2\epsilon$

This follows the same procedure as in the previous section, with the main difference being the appearance of  $J_{\diamond}^{(n)}(t)$ . Note the absence of  $E_4(2; t)$ , as remarked in sec. C.3.

$$E_4(4 - 2\epsilon; t) = \frac{1}{\epsilon^3} + \frac{14 - 9J_{\diamond}^{(1)}(t)}{6\epsilon^2} + \frac{t + 36 + 3\pi^2 - 51J_{\diamond}^{(1)}(t) + 9J_{\diamond}^{(2)}(t)}{12\epsilon} + \bar{E}_4(4; t) + \mathcal{O}(\epsilon),\quad (\text{D.17})$$

with the finite piece

$$\begin{aligned}\bar{E}_4(4; t) = & \frac{t^2 - 20t + 160}{96} E_1(2; t) - \frac{(t^2 - 28t + 120)(t - 16)}{96} E_2(2; t) \\ & - \frac{(t - 4)(t - 16)^2}{48} E_3(2; t) + \frac{25t - 136 + 14\pi^2}{24} - \zeta(3) - \frac{59 + 3\pi^2}{8} J_{\diamond}^{(1)}(t) + \frac{17}{8} J_{\diamond}^{(2)}(t) - \frac{1}{4} J_{\diamond}^{(3)}(t).\end{aligned}\quad (\text{D.18})$$

### D.6 The master integral $E_5$ in $d = 4 - 2\epsilon$

The expansion of the elliptic master integral  $E_5$  is more subtle, because a direct application of the dimension shifting relation derived in sec. C.4 gives  $1/\epsilon^2$  and  $1/\epsilon$  poles depending on the elliptic master integrals in  $d = 2$ . But the presence of the elliptic master integrals would spoil the renormalizability of the amplitude. These unwanted contributions are removed using the Schouten relations derived in sec. A.3. After using these identities, the  $\epsilon$  expansion reads

$$E_5(4 - 2\epsilon; t) = \frac{1}{3\epsilon^3} + \frac{1 - 3J_{\diamond}^{(1)}(t)}{3\epsilon^2} + \frac{[J_{\diamond}^{(1)}(t)]^2 - J_{\diamond}^{(1)}(t) + \frac{1}{2}J_{\diamond}^{(2)}(t) + \frac{\pi^2}{12} + \frac{1}{3}}{\epsilon} + \bar{E}_5(4; t) + \mathcal{O}(\epsilon).\quad (\text{D.19})$$

Unfortunately,  $\bar{E}_5(4; t)$  is not simply a combination of  $E_n(2; t)$  [as is the case for  $\bar{E}_1(4; t)$ , etc.] but also of various  $\bar{E}_n^{(r)}(2; t)$ . This can possibly be simplified using additional Schouten relations, the derivation of which would itself be a daunting task, and  $E_5(2; t)$  is also not easy to obtain. Instead, we use  $\bar{E}_5(4; t)$  as-is and evaluate it by solving its differential equation in terms of  $E_1(2; t)$ .

Rewritten in terms of  $\beta$  such that  $\beta^2 = 1 - 4/t$ , the finite piece of the differential equation eq. (B.9) is<sup>25</sup>

$$\beta^2 \left[ \frac{\partial^2}{\partial \beta^2} - \frac{2}{\beta^2 - 1} \right] \bar{E}_5(4; \beta) = \mathcal{S}_5(\beta).\quad (\text{D.20})$$

<sup>25</sup>Note that in this section,  $E_n(d; t)$  and  $E_n(d; \beta)$  are two different functions related by  $t = 4/(1 - \beta^2)$ . In general, when the kinematic argument of  $E_n$  (or  $J_{\diamond}^{(n)}$ , etc.) is a Greek letter, it plays the role of  $\beta$ , not  $t$ .

Serendipitously, the first-order term vanishes. The source term  $\mathcal{S}_5$  contains  $\bar{E}_1(4; t)$ ,  $\bar{E}_4(4; t)$  and their derivatives, but since eqs. (D.12) and (D.18) expresses these solely in terms of  $E_1(2; t)$  and  $J_{\circlearrowleft}^{(n)}(t)$ , we have the decomposition

$$\mathcal{S}_5(\beta) = \mathcal{S}_{\text{rat}}(\beta) + \mathcal{S}_J(\beta) + \mathcal{S}_{E_1}(\beta) \quad (\text{D.21})$$

with rational piece

$$\mathcal{S}_{\text{rat}}(\beta) := \frac{68\beta^4 - 44\beta^2 + 24 - \beta^2(\beta^2 + 5)\pi^2}{6(\beta^2 - 1)^2} + \frac{2\beta^2\zeta(3)}{3(\beta^2 - 1)}, \quad (\text{D.22})$$

$J_{\circlearrowleft}^{(n)}$ -dependent (i.e., polylogarithmic) piece

$$\begin{aligned} \mathcal{S}_J(\beta) := & \frac{\beta^2}{3(\beta^2 - 1)} J_{\circlearrowleft}^{(3)}(\beta) + \frac{2}{\beta^2 - 1} J_{\circlearrowleft}^{(1)}(\beta) J_{\circlearrowleft}^{(2)}(\beta) - \frac{\beta^4 + 5}{(\beta^2 - 1)^2} J_{\circlearrowleft}^{(2)}(\beta) - \frac{12}{(\beta^2 - 1)^2} J_{\circlearrowleft}^{(1)}(\beta)^2 \\ & + \frac{(\pi^2 - 4)\beta^4 + (8 - \pi^2)\beta^2 - 52}{2(\beta^2 - 1)^2} J_{\circlearrowleft}^{(1)}(\beta), \end{aligned} \quad (\text{D.23})$$

and  $E_1$ -dependent (i.e., elliptic) piece

$$\begin{aligned} \mathcal{S}_{E_1} &:= \left[ s_2(\beta) \frac{\partial^2}{\partial \beta^2} + s_1(\beta) \frac{\partial}{\partial \beta} + s_0(\beta) \right] E_1(2; \beta), \\ s_0(\beta) &= \frac{2}{3} \frac{\beta^2(2\beta^2 - 1)}{(\beta^2 - 1)^2}, \quad s_1(\beta) = \frac{2\beta}{3} \frac{3\beta^4 - 7\beta^2 + 3}{\beta^2 - 1}, \quad s_2(\beta) = \frac{\beta^2(4\beta^2 - 3)}{2}. \end{aligned} \quad (\text{D.24})$$

We solve this differential equation using the Wronskian method. A basis of solutions to the homogeneous equation [i.e., that obtained by setting  $\mathcal{S}_5(\beta) = 0$  in eq. (D.20)] is

$$g_1(\beta) := \beta^2 - 1 \quad \text{and} \quad g_2(\beta) := \frac{\beta^2 - 1}{4} \log \left( \frac{\beta + 1}{\beta - 1} \right) - \frac{\beta}{2}, \quad (\text{D.25})$$

and the generic solution is then

$$\bar{E}_5(4; \beta) = c_1 g_1(\beta) + c_2 g_2(\beta) - g_1(\beta) \int_{\xi_1}^{\beta} \mathcal{S}_5(\xi) g_2(\xi) \frac{d\xi}{\xi^2} + g_2(\beta) \int_{\xi_2}^{\beta} \mathcal{S}_5(\xi) g_1(\xi) \frac{d\xi}{\xi^2}. \quad (\text{D.26})$$

The limits  $\xi_1$  and  $\xi_2$  are arbitrary as long as the constants  $c_1$  and  $c_2$  are adjusted accordingly, which can be done by ensuring that the  $\beta = \infty$  (i.e.,  $t = 0$ ) limit from sec. B.5 is reproduced. Such adjustment is very subtle in practice, and one particular implementation will be discussed in forthcoming work [39].

The elliptic piece would be simpler if it only involved  $E_1$ , not its derivatives, so we apply integration by parts. Defining

$$h_n(\xi) := \frac{\partial^2}{\partial \xi^2} \frac{s_2(\xi) g_n(\xi)}{\xi^2} - \frac{\partial}{\partial \xi} \frac{s_1(\xi) g_n(\xi)}{\xi^2} + \frac{s_0(\xi) g_n(\xi)}{\xi^2}, \quad (\text{D.27})$$

or, explicitly,

$$h_1(\xi) = \frac{54\xi^6 - 57\xi^4 + 11\xi^2 - 6}{3\xi^2(\xi^2 - 1)}, \quad (\text{D.28})$$

$$h_2(\xi) = \frac{(\xi^2 - 1)(54\xi^6 - 57\xi^4 + 11\xi^2 - 6) \log\left(\frac{\xi+1}{\xi-1}\right) - 2\xi(54\xi^6 - 93\xi^4 + 31\xi^2 + 6)}{12(\xi^2 - 1)^2\xi^2},$$

we have

$$\begin{aligned} & g_2(\beta) \int_{\xi_2}^{\beta} \mathcal{S}_{E_1}(\xi) g_1(\xi) \frac{d\xi}{\xi^2} - g_1(\beta) \int_{\xi_1}^{\beta} \mathcal{S}_{E_1}(\xi) g_2(\xi) \frac{d\xi}{\xi^2} \\ &= g_2(\beta) \int_{\xi_2}^{\beta} h_1(\xi) E_1(2; \xi) d\xi - g_1(\beta) \int_{\xi_1}^{\beta} h_2(\xi) E_1(2; \xi) d\xi + \frac{s_2(\beta)}{\beta^2} E_1(2; \beta) + \Delta_{E_1}, \quad (\text{D.29}) \end{aligned}$$

where  $\Delta_{E_1}$  incorporates all boundary terms from the lower integration limit; we will omit it from now on since it can be absorbed into  $c_1 g_1(\beta) + c_2 g_2(\beta)$ . At the upper integration limit, all boundary terms cancel except for  $\frac{s_2(\beta)}{\beta^2} [g_1(\beta)g'_2(\beta) - g'_1(\beta)g_2(\beta)] E_1(2; \beta)$ , where the factor in brackets is equal to 1.

For brevity in the following, we define

$$\begin{aligned} \mathcal{I}[\beta; G_1, G_2] &:= -G_1 \int_{\xi_1}^{\beta} \left[ \frac{\mathcal{S}_J(\xi) + \mathcal{S}_{\text{rat}}(\xi)}{\xi^2} g_2(\xi) + E_1(2; \xi) h_2(\xi) \right] d\xi \\ &\quad + G_2 \int_{\xi_2}^{\beta} \left[ \frac{\mathcal{S}_J(\xi) + \mathcal{S}_{\text{rat}}(\xi)}{\xi^2} g_1(\xi) + E_1(2; \xi) h_1(\xi) \right] d\xi. \end{aligned} \quad (\text{D.30})$$

The reason for introducing  $G_1, G_2$  will become apparent in eq. (D.35). Thus,

$$\bar{E}_5(4; \beta) = c_1 g_1(\beta) + c_2 g_2(\beta) + \frac{s_2(\beta)}{\beta^2} E_1(2; \beta) + \mathcal{I}[\beta; g_1(\beta), g_2(\beta)]. \quad (\text{D.31})$$

While this form of  $E_5(4; \beta)$  involving a one-dimensional integral is much more tractable than the original 12-dimensional Feynman integral, the evaluation of  $\mathcal{I}[\beta; G_1, G_2]$  is a formidable task in and of itself, not least because it depends on the ability to evaluate  $E_1(2; \xi)$  across the entire integration range. This is detailed in forthcoming work [39].

## D.7 The master integral $E_6$ at $d = 4 - 2\epsilon$

As for  $E_5$ , the Schouten relations must be applied to the  $\epsilon$  expansion of this integral. After doing that, it reads

$$E_6(4 - 2\epsilon; t) = \frac{2 + J_{\infty}^{(1)}(t) - 4[J_{\infty}^{(1)}(t)]^2 + 10J_{\infty}^{(1)}(t) + J_{\infty}^{(2)}(t) - 4}{2(t - 4)\epsilon^2} + \bar{E}_6(4; t) + \mathcal{O}(\epsilon), \quad (\text{D.32})$$

where, using the relation eq. (B.12),

$$\begin{aligned} \bar{E}_6(4; t) &= \left[ \frac{t - 16}{48} \frac{\partial^2}{\partial t^2} - \frac{t + 16}{24t} \frac{\partial}{\partial t} + \frac{1}{24t} \right] \bar{E}_1(4; t) + \frac{\bar{E}_4(4; t)}{2t} - \left[ \frac{\partial}{\partial t} + \frac{1}{t} \right] \bar{E}_5(4; t) \\ &\quad + \frac{2J_{\infty}^{(3)}(t) - 39J_{\infty}^{(2)}(t) + 3(\pi^2 + 67)J_{\infty}^{(1)}(t)}{48t} + \frac{8\zeta(3) - 11\pi^2}{32t} + \frac{3t^2 - 184t - 5490}{1728t}, \end{aligned} \quad (\text{D.33})$$

or in terms of  $E_1(2; t)$  using the expression for  $\bar{E}_4(4; t)$  in eq. (D.18)

$$\begin{aligned}\bar{E}_6(4; t) = & \left[ \frac{(t-16)(t-4)}{12t^2} \left( t \frac{\partial}{\partial t} \right)^2 + \frac{t-10}{12t} t \frac{\partial}{\partial t} + \frac{1}{24} \right] E_1(2; t) - \left[ \frac{\partial}{\partial t} + \frac{1}{t} \right] \bar{E}_5(4; t) \\ & + \frac{-4J_{\infty}^{(3)}(t) + 12J_{\infty}^{(2)}(t) + 6(4-\pi^2)J_{\infty}^{(1)}(t)}{48t} - \frac{\zeta(3)+5}{3t} + \frac{\pi^2}{12t},\end{aligned}\quad (\text{D.34})$$

where in the second form we have used eqs. (D.12) and (D.18) to express everything in terms of  $E_1(2; t)$ ,  $\bar{E}_5(4; t)$  and  $J_{\infty}^{(n)}(t)$ . The derivative of  $\bar{E}_5(4; t)$  can be extracted via  $\frac{\partial}{\partial t} = \frac{(\beta^2-1)^2}{8\beta} \frac{\partial}{\partial \beta}$ , eq. (D.19) and eq. (D.31):

$$\begin{aligned}\frac{\partial \bar{E}_5(4; t)}{\partial t} = & \left[ \frac{t-16}{2t} \frac{\partial}{\partial t} + \frac{t^2-28t+48}{3t^2(t-4)} \right] E_1(2; t) \\ & + \frac{(\beta^2-1)^2}{8\beta} \left( 2\beta c_1 + \frac{1}{2} J_{\infty}^{(1)}(\beta) c_2 + \mathcal{I}[\beta; 2\beta, \frac{1}{2} J_{\infty}^{(1)}(\beta)] \right),\end{aligned}\quad (\text{D.35})$$

where the integral function  $\mathcal{I}$  is the same as in eq. (D.30). As for  $\bar{E}_5$ , the remainder of the calculation is deferred to forthcoming work [39].

## E Expressions for the master integrals in two dimensions

At this point, all master integrals have been rewritten in terms of  $J_{\infty}^{(n)}(t)$  (given in sec. D.2) and  $E_1(2; t)$ , so it remains to describe this ‘‘master of master integrals’’. It has been extensively studied and is known in several different forms, among which is the Bessel integral representation [25, 31, 32], which holds for  $t < 16$ :

$$E_1(2; t) = -8 \int_0^\infty x I_0(x\sqrt{t}) [K_0(x)]^4 dx, \quad (\text{E.1})$$

where  $I_\alpha(z)$  and  $K_\alpha(z)$  are the modified Bessel functions of the first and second kind, respectively. This has as a special case  $E_0(2) = E_1(2; 0) = 7\zeta(3)$ .

Combining eq. (E.1) with eqs. (B.6) and (B.7) gives

$$E_2(2; t) = 2 \int_0^\infty x \left\{ I_0(x\sqrt{t}) + \frac{x\sqrt{t}}{2} I_1(x\sqrt{t}) \right\} [K_0(x)]^4 dx, \quad (\text{E.2})$$

$$E_3(2; t) = -\frac{1}{2} \int_0^\infty x \left\{ (2+x^2) I_0(x\sqrt{t}) + \frac{x(t+2)}{\sqrt{t}} I_1(x\sqrt{t}) + x^2 I_2(x\sqrt{t}) \right\} [K_0(x)]^4 dx. \quad (\text{E.3})$$

When  $t < 0$ , the integrals are kept real by  $\sqrt{t} = i\sqrt{|t|}$  and  $I_\alpha(iz) = i^\alpha J_\alpha(z)$ , where  $J_\alpha$  is the (unmodified) Bessel function of the first kind.

The Bessel integral formulation is straightforward, but it is limited to  $t < 16$  and is numerically rather slow. The formulation in terms of elliptic functions that is the main result of ref. [32] is applicable everywhere in the complex plane, but is much more complicated to describe, requiring much higher mathematics than what is used elsewhere in this paper. They are also given in terms of variables whose relationship to our  $t$  is highly non-trivial, and, while known in the literature [32], require adjustments before being practical. To keep the scope of the present paper manageable, we therefore defer its description to forthcoming work [39].

## F Unsubtracted expressions for the HVP

Only the on-shell renormalized result  $\bar{\Pi}_T(q^2) := \Pi_T(q^2) - \Pi_T(0)$  is presented in the main text, but for completeness, we give the unsubtracted result  $\Pi_T(q^2)$  in this appendix. Arranging the chiral power counting as in eq. (4.1), the lower-order expressions [compare eqs. (4.2) and (4.3)] are

$$\Pi_T^{\text{NLO}}(t) = 2 \left[ \frac{4-t}{3t} J_{\infty}^{(1)}(t) - \frac{1+3L_{\pi}}{9} \right] - 4l_5^q - 8h_2^q, \quad (\text{F.1})$$

$$\begin{aligned} \Pi_T^{\text{NNLO}}(t) = t \left[ \frac{4-t}{3t} J_{\infty}^{(1)}(t) - \frac{1+3L_{\pi}}{9} \right]^2 - 4t \left[ \frac{4-t}{3t} J_{\infty}^{(1)}(t) - \frac{1+3L_{\pi}}{9} \right] l_6^q \\ + 8L_{\pi}(2l_5^q - l_6^q) - 8tc_{56}^q - 32c_{34}^q. \end{aligned} \quad (\text{F.2})$$

For the N<sup>3</sup>LO expression, we use the same thematic subdivision as in eq. (4.4):

$$\Pi_T^{\text{N}^3\text{LO}}(t) = \Pi_E(t) + \Pi_J(t) + \Pi_l(t) + \Pi_c(t) + \Pi_{\zeta}(t) + r_0^q + tr_1^q + t^2r_2^q. \quad (\text{F.3})$$

Due to how the contributions are subdivided,  $\Pi_E(t) = \bar{\Pi}_E(t)$  and  $\Pi_J(t) = \bar{\Pi}_J(t)$  [see eqs. (4.5) and (4.6)]. For the remaining parts, we have

$$\Pi_l(t) = \bar{\Pi}_l(t) - 4L_{\pi}^2(2l_1^q - l_2^q + 12l_5^q - 6l_6^q) + \frac{2-4L_{\pi}}{3}(l_1^q + 2l_2^q) + 16L_{\pi}l_4^q(2l_5^q - l_6^q), \quad (\text{F.4})$$

$$\begin{aligned} \Pi_c(t) = \bar{\Pi}_c(t) - \left( 192c_6^q + 48c_{29}^q - 16c_{30}^q + 12c_{31}^q + 12c_{32}^q - 8c_{33}^q \right. \\ \left. - 192c_{34}^q + 32c_{35}^q - 32c_{44}^q + 64c_{46}^q - 128c_{47}^q + 32c_{50}^q \right) L_{\pi} \\ + 6c_{31}^q + 6c_{32}^q - 4c_{33}^q - 16c_{44}^q + 64(l_3^q - l_4^q)c_{34}^q, \end{aligned} \quad (\text{F.5})$$

$$\begin{aligned} \Pi_{\zeta}(t) = -\frac{3t^2 - 13t - 6}{27t}\zeta(3) - \frac{t^2 + 18t}{81}L_{\pi}^3 - \frac{20t - 207}{27}L_{\pi}^2 - \left[ \frac{17t^2}{432} - \frac{845t}{648} + \frac{703}{54} \right] L_{\pi} \\ - \left[ \frac{t^2}{216} - \frac{5t}{27} + \frac{22}{27} + \frac{1}{18t} \right] \pi^2 + \frac{20245t^2}{139968} - \frac{55511t}{23328} - \frac{65195}{3888} + \frac{1216}{27t}. \end{aligned} \quad (\text{F.6})$$

In order to obtain the physical result presented in sec. 4, the  $t \rightarrow 0$  limit of the above expressions must be taken and subtracted. For small  $t$ ,  $J_{\infty}^{(2)}(t) = \mathcal{O}(t^2)$  and  $J_{\infty}^{(3)}(t) = \mathcal{O}(t^3)$ , so these functions do not contribute [see eq. (D.7)]. However,  $J_{\infty}^{(1)}(t) = -\frac{t}{6} + \mathcal{O}(t^2)$ , so we have

$$\Pi_T^{\text{NLO}}(0) = -\frac{5+3L_{\pi}}{9} - 4l_5^q - 8h_2^q, \quad \Pi_T^{\text{NNLO}}(0) = 8L_{\pi}(2l_5^q - l_6^q) - 32c_{34}^q, \quad (\text{F.7})$$

$$\Pi_J(0) = \frac{4-\pi^2}{36}. \quad (\text{F.8})$$

For N<sup>3</sup>LO, we also need the expansion eq. (B.16) of the elliptic master integrals. This gives

$$\Pi_E(t) = -\left[ \frac{1216}{27} + \frac{2\zeta(3)}{9} - \frac{\pi^2}{18} \right] \frac{1}{t} + \left[ \frac{52069}{1944} - \frac{7957\zeta(3)}{432} + \frac{91\pi^2}{108} \right] + \mathcal{O}(t), \quad (\text{F.9})$$

whose pole cancels against that of  $\Pi_{\zeta}(t)$ . Subtracting  $\Pi_J(0)$  and the finite part of  $\Pi_E(t)$  from  $\Pi_{\zeta}(0)$  produces  $\bar{\Pi}_{\zeta}(t)$ .

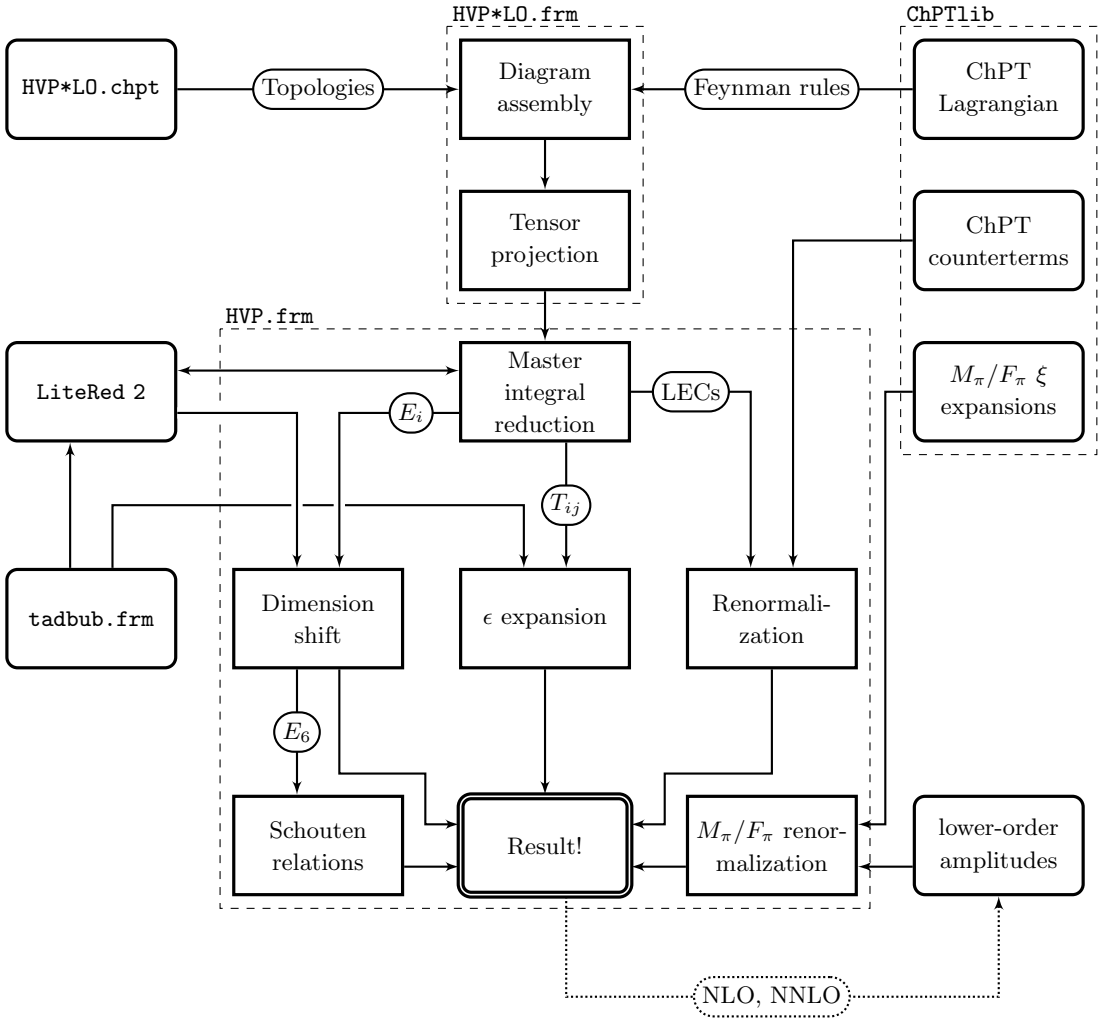


**Figure 2:** A sketch of the steps involved in the HVP calculations, and the programs performing these steps. For NLO and NNLO, only a subset of the steps are of course performed. With the exception of third-party programs like FORM [43, 44] and LiteRed 2 [49, 50], all necessary code can be found in the linked repositories [71, 72].

## G Implementation details

The calculation of the amplitude was carried out using the FORM library ChPTlib [71], which during the preparation of this work evolved from Mattias Sjö's personal FORM files (themselves inspired by Johan Bijnens' ditto) into something more generally usable (albeit still limited and under development). We therefore choose to make it available, along with the implementation of the present HVP calculation [72], so that the reader may reproduce our results. In this appendix, we briefly describe how to do that. A graphical outline is given in fig. 2, and a step-by-step summary in the provided README file.<sup>26</sup>

<sup>26</sup>Questions regarding the implementation should primarily be directed to Mattias Sjö.

`ChPTlib` is mainly a collection of `FORM` procedures, containing an implementation of the bare and renormalized ChPT Lagrangian [6, 7, 17, 45, 46] and utilities for processing ChPT amplitudes. It also contains a Python program `ChPT.py` for automatically generating the necessary `FORM` code given a description of the diagram topologies (it is currently not interoperable with automatic Feynman diagram generators). The diagram description format is intended to be quickly transcribed by hand from a sketch of the diagrams, and to express the momentum routing in a way that directly translates into the  $I_{\vec{\nu}}$  notation of sec. 3. The diagrams in tables 1 and 2 are found in this format in `HVP*LO.chpt` (with \* standing for N, NN or N3), and running `ChPT.py --form HVP*LO.chpt` generates the `FORM` code for deriving the Feynman rules, performing all Wick contractions, and symmetrizing. This is then applied by running the `FORM` program `HVP*LO.frm`, which is generated with `ChPT.py --form-main HVP*LO.chpt` and then supplanted with, among other things, an implementation of eq. (2.3).

With the diagrams generated, all subsequent steps in the calculation are performed by running the `FORM` program `HVP.frm`. The most time-consuming step is the master integral reduction, which is done by converting the raw amplitude into a `Mathematica` program that invokes `LiteRed 2` [49, 50], running it, and converting the result back to `FORM`. After that, the other manipulations described in sec. 3 are performed as outlined in fig. 2. Of particular note is the standalone file `tadbub.frm`, which broadcasts the  $\epsilon$ -expansion (see sec. D.2) of the tadpole and bubble integrals, thereby minimizing the risk of clashes between sign and normalization conventions in the various places where this expansion is needed. The output of `HVP.frm` is only some `LATEX` formatting away from eqs. (4.2) to (4.9), and most of the crosschecks listed in sec. 4 can be automatically performed by setting various flags listed at the top of the file.

## References

- [1] MUON G-2 collaboration, D. P. Aguillard et al., *Measurement of the Positive Muon Anomalous Magnetic Moment to 127 ppb*, [2506.03069](#).
- [2] FCC collaboration, A. Abada et al., *FCC Physics Opportunities: Future Circular Collider Conceptual Design Report Volume 1*, *Eur. Phys. J. C* **79** (2019) 474.
- [3] R. Aliberti et al., *The anomalous magnetic moment of the muon in the Standard Model: an update*, [2505.21476](#).
- [4] A. Boccaletti et al., *High precision calculation of the hadronic vacuum polarisation contribution to the muon anomaly*, [2407.10913](#).
- [5] A. Keshavarzi, D. Nomura and T. Teubner,  *$g-2$  of charged leptons,  $\alpha(M_Z^2)$ , and the hyperfine splitting of muonium*, *Phys. Rev. D* **101** (2020) 014029 [[1911.00367](#)].
- [6] J. Gasser and H. Leutwyler, *Chiral Perturbation Theory to One Loop*, *Annals Phys.* **158** (1984) 142.
- [7] J. Gasser and H. Leutwyler, *Chiral Perturbation Theory: Expansions in the Mass of the Strange Quark*, *Nucl. Phys. B* **250** (1985) 465.
- [8] M. T. Hansen and A. Patella, *Finite-volume effects in  $(g-2)_\mu^{\text{HVP,LO}}$* , *Phys. Rev. Lett.* **123** (2019) 172001 [[1904.10010](#)].

[9] M. T. Hansen and A. Patella, *Finite-volume and thermal effects in the leading-HVP contribution to muonic  $(g-2)$* , *JHEP* **10** (2020) 029 [[2004.03935](#)].

[10] M. Lüscher, *Two particle states on a torus and their relation to the scattering matrix*, *Nucl. Phys. B* **354** (1991) 531.

[11] L. Lellouch and M. Lüscher, *Weak transition matrix elements from finite volume correlation functions*, *Commun. Math. Phys.* **219** (2001) 31 [[hep-lat/0003023](#)].

[12] H. B. Meyer, *Lattice QCD and the Timelike Pion Form Factor*, *Phys. Rev. Lett.* **107** (2011) 072002 [[1105.1892](#)].

[13] C. Aubin, T. Blum, M. Golterman and S. Peris, *Application of effective field theory to finite-volume effects in  $a_\mu^{\text{HVP}}$* , *Phys. Rev. D* **102** (2020) 094511 [[2008.03809](#)].

[14] C. Aubin, T. Blum, P. Chau, M. Golterman, S. Peris and C. Tu, *Finite-volume effects in the muon anomalous magnetic moment on the lattice*, *Phys. Rev. D* **93** (2016) 054508 [[1512.07555](#)].

[15] C. Aubin, T. Blum, C. Tu, M. Golterman, C. Jung and S. Peris, *Light quark vacuum polarization at the physical point and contribution to the muon  $g-2$* , *Phys. Rev. D* **101** (2020) 014503 [[1905.09307](#)].

[16] S. Borsanyi et al., *Leading hadronic contribution to the muon magnetic moment from lattice QCD*, *Nature* **593** (2021) 51 [[2002.12347](#)].

[17] J. Bijnens, G. Colangelo and G. Ecker, *The Mesonic chiral Lagrangian of order  $p^6$* , *JHEP* **02** (1999) 020 [[hep-ph/9902437](#)].

[18] D. Djukanovic, G. von Hippel, S. Kuberski, H. B. Meyer, N. Miller, K. Ott nad et al., *The hadronic vacuum polarization contribution to the muon  $g-2$  at long distances*, *JHEP* **04** (2025) 098 [[2411.07969](#)].

[19] RBC, UKQCD collaboration, T. Blum et al., *Long-Distance Window of the Hadronic Vacuum Polarization for the Muon  $g-2$* , *Phys. Rev. Lett.* **134** (2025) 201901 [[2410.20590](#)].

[20] FERMILAB LATTICE, HPQCD, MILC collaboration, A. Bazavov et al., *Hadronic Vacuum Polarization for the Muon  $g-2$  from Lattice QCD: Long-Distance and Full Light-Quark Connected Contribution*, *Phys. Rev. Lett.* **135** (2025) 011901 [[2412.18491](#)].

[21] J. Bijnens, G. Colangelo and P. Talavera, *The Vector and scalar form-factors of the pion to two loops*, *JHEP* **05** (1998) 014 [[hep-ph/9805389](#)].

[22] J. Bijnens and N. Hermansson Truedsson, *The Pion Mass and Decay Constant at Three Loops in Two-Flavour Chiral Perturbation Theory*, *JHEP* **11** (2017) 181 [[1710.01901](#)].

[23] O. V. Tarasov, *Connection between Feynman integrals having different values of the space-time dimension*, *Phys. Rev. D* **54** (1996) 6479 [[hep-th/9606018](#)].

[24] S. Groote, J. G. Korner and A. A. Pivovarov, *On the evaluation of sunset - type Feynman diagrams*, *Nucl. Phys. B* **542** (1999) 515 [[hep-ph/9806402](#)].

[25] S. Groote, J. G. Korner and A. A. Pivovarov, *On the evaluation of a certain class of Feynman diagrams in  $x$ -space: Sunrise-type topologies at any loop order*, *Annals Phys.* **322** (2007) 2374 [[hep-ph/0506286](#)].

[26] D. J. Broadhurst, J. Fleischer and O. V. Tarasov, *Two loop two point functions with masses: Asymptotic expansions and Taylor series, in any dimension*, *Z. Phys. C* **60** (1993) 287 [[hep-ph/9304303](#)].

[27] R. N. Lee and A. I. Onishchenko,  *$\epsilon$ -regular basis for non-polylogarithmic multiloop integrals and total cross section of the process  $e^+e^- \rightarrow 2(Q\bar{Q})$* , *JHEP* **12** (2019) 084 [[1909.07710](#)].

[28] R. N. Lee and A. I. Onishchenko, *Master integrals for bipartite cuts of three-loop photon self energy*, *JHEP* **04** (2021) 177 [[2012.04230](#)].

[29] F. Forner, C. Nega and L. Tancredi, *On the photon self-energy to three loops in QED*, *JHEP* **03** (2025) 148 [[2411.19042](#)].

[30] J. Wang, X. Wang and Y. Wang, *Analytic decay width of the Higgs boson to massive bottom quarks at order  $\alpha_s^3$* , *JHEP* **03** (2025) 163 [[2411.07493](#)].

[31] D. H. Bailey, J. M. Borwein, D. Broadhurst and M. L. Glasser, *Elliptic integral evaluations of Bessel moments*, *J. Phys. A* **41** (2008) 205203 [[0801.0891](#)].

[32] S. Bloch, M. Kerr and P. Vanhove, *A Feynman integral via higher normal functions*, *Compos. Math.* **151** (2015) 2329 [[1406.2664](#)].

[33] A. Primo and L. Tancredi, *Maximal cuts and differential equations for Feynman integrals. An application to the three-loop massive banana graph*, *Nucl. Phys. B* **921** (2017) 316 [[1704.05465](#)].

[34] J. Broedel, C. Duhr, F. Dulat, R. Marzucca, B. Penante and L. Tancredi, *An analytic solution for the equal-mass banana graph*, *JHEP* **09** (2019) 112 [[1907.03787](#)].

[35] S. Pögel, X. Wang and S. Weinzierl, *The three-loop equal-mass banana integral in  $\varepsilon$ -factorised form with meromorphic modular forms*, *JHEP* **09** (2022) 062 [[2207.12893](#)].

[36] P. Lairez and P. Vanhove, *Algorithms for minimal Picard–Fuchs operators of Feynman integrals*, *Lett. Math. Phys.* **113** (2023) 37 [[2209.10962](#)].

[37] L. de la Cruz and P. Vanhove, *Algorithm for differential equations for Feynman integrals in general dimensions*, *Lett. Math. Phys.* **114** (2024) 89 [[2401.09908](#)].

[38] L. Tancredi, *Integration by parts identities in integer numbers of dimensions. A criterion for decoupling systems of differential equations*, *Nucl. Phys. B* **901** (2015) 282 [[1509.03330](#)].

[39] L. Lellouch, A. Lupo, M. Sjö and P. Vanhove, *The elliptic three-loop integrals of hadronic vacuum polarization in chiral perturbation theory*, to appear.

[40] E. Golowich and J. Kambor, *Two loop analysis of vector current propagators in chiral perturbation theory*, *Nucl. Phys. B* **447** (1995) 373 [[hep-ph/9501318](#)].

[41] G. Amoros, J. Bijnens and P. Talavera, *Two point functions at two loops in three flavor chiral perturbation theory*, *Nucl. Phys. B* **568** (2000) 319 [[hep-ph/9907264](#)].

[42] J. Bijnens and J. Lu, *Two-Point Functions and S-Parameter in QCD-like Theories*, *JHEP* **01** (2012) 081 [[1111.1886](#)].

[43] J. A. M. Verma, *New features of FORM*, [math-ph/0010025](#).

[44] B. Ruijl, T. Ueda and J. Vermaseren, *FORM version 4.2*, [1707.06453](#).

[45] J. Bijnens, G. Colangelo and G. Ecker, *Renormalization of chiral perturbation theory to order  $p^6$* , *Annals Phys.* **280** (2000) 100 [[hep-ph/9907333](#)].

[46] J. Bijnens, N. Hermansson-Truedsson and S. Wang, *The order  $p^8$  mesonic chiral Lagrangian*, *JHEP* **01** (2019) 102 [[1810.06834](#)].

[47] J. Bijnens and G. Ecker, *Mesonic low-energy constants*, *Ann. Rev. Nucl. Part. Sci.* **64** (2014) 149 [[1405.6488](#)].

[48] U. Burgi, *Charged pion pair production and pion polarizabilities to two loops*, *Nucl. Phys. B* **479** (1996) 392 [[hep-ph/9602429](#)].

[49] R. N. Lee, *Presenting LiteRed: a tool for the Loop InTEgrals REDuction*, [1212.2685](#).

[50] R. N. Lee, *LiteRed 1.4: a powerful tool for reduction of multiloop integrals*, *J. Phys. Conf. Ser.* **523** (2014) 012059 [[1310.1145](#)].

[51] S. Borowka, G. Heinrich, S. Jahn, S. P. Jones, M. Kerner, J. Schlenk et al., *pySecDec: a toolbox for the numerical evaluation of multi-scale integrals*, *Comput. Phys. Commun.* **222** (2018) 313 [[1703.09692](#)].

[52] S. Borowka, G. Heinrich, S. Jahn, S. P. Jones, M. Kerner and J. Schlenk, *A GPU compatible quasi-Monte Carlo integrator interfaced to pySecDec*, *Comput. Phys. Commun.* **240** (2019) 120 [[1811.11720](#)].

[53] G. Heinrich, S. Jahn, S. P. Jones, M. Kerner, F. Langer, V. Magerya et al., *Expansion by regions with pySecDec*, *Comput. Phys. Commun.* **273** (2022) 108267 [[2108.10807](#)].

[54] G. Heinrich, S. P. Jones, M. Kerner, V. Magerya, A. Olsson and J. Schlenk, *Numerical scattering amplitudes with pySecDec*, *Comput. Phys. Commun.* **295** (2024) 108956 [[2305.19768](#)].

[55] K. Melnikov and T. van Ritbergen, *The Three loop on-shell renormalization of QCD and QED*, *Nucl. Phys. B* **591** (2000) 515 [[hep-ph/0005131](#)].

[56] J. Bijnens, T. Husek and M. Sjö, *Six-meson amplitude in QCD-like theories*, *Phys. Rev. D* **106** (2022) 054021 [[2206.14212](#)].

[57] NA7 collaboration, S. R. Amendolia et al., *A Measurement of the Space - Like Pion Electromagnetic Form-Factor*, *Nucl. Phys. B* **277** (1986) 168.

[58] B. Ananthanarayan, I. Caprini, D. Das and I. Sentitemsu Imsong, *Parametrisation-free determination of the shape parameters for the pion electromagnetic form factor*, *Eur. Phys. J. C* **73** (2013) 2520 [[1302.6373](#)].

[59] T. P. Leplumey and P. Stoffer, *Dispersive analysis of the pion vector form factor without zeros*, [2501.09643](#).

[60] V. Smirnov, *Analytic Tools for Feynman Integrals*, Springer Tracts in Modern Physics. Springer Berlin Heidelberg, 2013.

[61] G. Travaglini et al., *The SAGEX review on scattering amplitudes*, *J. Phys. A* **55** (2022) 443001 [[2203.13011](#)].

[62] S. Laporta, *High-precision calculation of multiloop Feynman integrals by difference equations*, *Int. J. Mod. Phys. A* **15** (2000) 5087 [[hep-ph/0102033](#)].

[63] A. V. Smirnov and A. V. Petukhov, *The Number of Master Integrals is Finite*, *Lett. Math. Phys.* **97** (2011) 37 [[1004.4199](#)].

[64] R. N. Lee and A. A. Pomeransky, *Critical points and number of master integrals*, *JHEP* **11** (2013) 165 [[1308.6676](#)].

[65] T. Bitoun, C. Bogner, R. P. Klausen and E. Panzer, *Feynman integral relations from parametric annihilators*, *Lett. Math. Phys.* **109** (2019) 497 [[1712.09215](#)].

[66] N. Nakanishi, *Graph Theory and Feynman Integrals*. Gordon and Breach, 1971.

- [67] E. Remiddi and L. Tancredi, *Schouten identities for Feynman graph amplitudes; The Master Integrals for the two-loop massive sunrise graph*, *Nucl. Phys. B* **880** (2014) 343 [[1311.3342](https://arxiv.org/abs/1311.3342)].
- [68] “NIST Digital Library of Mathematical Functions.” <https://dlmf.nist.gov/>, Release 1.2.4 of 2025-03-15.
- [69] E. Panzer, *Algorithms for the symbolic integration of hyperlogarithms with applications to Feynman integrals*, *Comput. Phys. Commun.* **188** (2015) 148 [[1403.3385](https://arxiv.org/abs/1403.3385)].
- [70] S. L. Cacciatori, H. Epstein and U. Moschella, *Banana integrals in configuration space*, *Nucl. Phys. B* **995** (2023) 116343 [[2304.00624](https://arxiv.org/abs/2304.00624)].
- [71] <https://github.com/mssjo/ChPTlib>
- [72] <https://github.com/mssjo/HVP-3loop>